PRECURSORS TO PP

D. W. King, et al

Royal Norwegian Council for Scientific and Industrial Research

Prepared for:

Air Force Technical Applications Center
Advanced Research Projects Agency

28 February 1975

REPORT DOCUMENTATION PAGE

READ INSTRUCTIONS BEFORE COMPLETING FORM

1. REPORT NUMBER: F08606-74-C-0049	2. GOVT ACCESSION NO.
3. RECIPIENT'S CATALOG NUMBER: AD-A008 180	
4. TITLE (and Subtitle): Precursors to PP	5. TYPE OF REPORT & PERIOD COVERED: One-time technical
6. PERFORMING ORG. REPORT NUMBER: Scientific Rep. 3-74/75	
7. AUTHOR(s): D.W. King[1], R.A.W. Haddon[2] and E.S. Husebye[1]	8. CONTRACT OR GRANT NUMBER(s): F08606-74-C-0049
9. PERFORMING ORGANIZATION NAME AND ADDRESS: 1) NTNF/NORSAR, 2007 Kjeller, Norway; 2) Dept. of Applied Math., University of Sydney, Australia	10. PROGRAM ELEMENT, PROJECT, TASK AREA & WORK UNIT NUMBERS: NORSAR Phase 3
11. CONTROLLING OFFICE NAME AND ADDRESS: VELA Seismological Center, 312 Montgomery Street, Alexandria, Virginia 22314	12. REPORT DATE: 28 February 1975
	13. NUMBER OF PAGES: 62
14. MONITORING AGENCY NAME & ADDRESS (if different from Controlling Office)	15. SECURITY CLASS. (of this report)
	15a. DECLASSIFICATION/DOWNGRADING SCHEDULE

16. DISTRIBUTION STATEMENT (of this Report)

APPROVED FOR PUBLIC RELEASE, DISTRIBUTION UNLIMITED.

17. DISTRIBUTION STATEMENT (of the abstract entered in Block 20, if different from Report)

18. SUPPLEMENTARY NOTES

19. KEY WORDS (Continue on reverse side if necessary and identify by block number)

Precursors to PP, Seismic wave scattering, P coda, crust and upper mantle structure.

20. ABSTRACT (Continue on reverse side if necessary and identify by block number)

The results of a theoretical study of the interpretation of precursors to PP ($\Delta \sim 100^{\circ}$) in terms of scattering by small-scale random irregularities in the crust and uppermost mantle are presented. These results are compared with observational data from 2 nuclear explosions recorded at the Warramunga array and 3 earthquakes recorded at the NORSAR array. This comparison reveals that the scattering interpretation offers a plausible and adequate explanation of the detailed observational data, namely: onset times, duration, slowness, azimuth and amplitude variations. The scattering interpretation of PP precursors

along with a similar interpretation of precursors to PKPPKP, removes the need for postulating sharp reflecting discontinuities in the uppermost few hundred kilometers of the crust and upper mantle.

AFTAC Project Authorization No.:		VT/5702/B/ETR
ARPA Order No.	:	2551
Program Code No.	:	5F10
Name of Contractor	:	Royal Norwegian Council for Scientific and Industrial Research
Effective Date of Contract	:	1 July 1974
Contract Expiration Date	:	30 June 1975
Contract No.	:	F08606-74-C-0049
Project Manager	:	Nils Marås (02) 71 69 15
Title of Work	:	Norwegian Seismic Array (NORSAR) Phase 3
Amount of Contract	:	$900 000
Contract period covered by the report	:	1 July - 30 June 1974

This research was supported by the Advanced Research Projects Agency of the Department of Defense and was monitored by AFTAC/VSC, Patrick AFB FL 32925, under Contract No. F08606-74-C-0049.

CONTENTS

ABSTRACT

The results of a theoretical study of the interpretation of precursors to PP ($\Delta \sim 100^{\circ}$) in terms of scattering by small-scale random irregularities in the crust and uppermost mantle are presented. These results are compared with observational data from 2 nuclear explosions recorded at the Warramunga array and 3 earthquakes recorded at the NORSAR array. This comparison reveals that the scattering interpretation offers a plausible and adequate explanation of the detailed observational data, namely: onset times, duration, slowness, azimuth and amplitude variations. The scattering interpretation of PP precursors, along with a similar interpretation of precursors to PKPPKP, removes the need for postulating sharp reflecting discontinuities in the uppermost few hundred kilometers of the crust and upper mantle.

1 INTRODUCTION

The use of spatial arrangements of seismometers has contributed greatly to detailed investigations of Earth structure for more than a decade. Of particular importance has been the ability to obtain estimates of slowness (s) and azimuth (Φ) directly from array data. Such estimates are inherently more satisfactory than indirect estimates (e.g., from smoothed travel time observations) and have been mainly responsible for recent advances in knowledge of the P (and S) velocity distributions both with depth and laterally inside the Earth. Direct (s,Φ) estimates recently acquired a new significance with the advent of the interpretation of certain seismic signals in terms of scattering by random inhomogeneities. For scattered signals, slowness (which, as usual, refers to slowness or ray parameter of an arrival at the receiver) will not generally be the same as the gradient ($dT/d\Delta$) of an associated travel time (T,Δ) curve, and must therefore be measured directly. In addition, scattered waves will generally arrive at a receiver simultaneously from a range of different directions, and so reliable estimates of the slownesses and azimuths of the various contributions must by necessity involve the use of seismic arrays.

In this paper array estimates of (s,Φ) are brought to bear in a critical analysis of an interpretation of the so-called precursors to PP in terms of scattering by small-scale

random inhomogeneities in the Earth's crust and upper mantle recently proposed by Cleary and Haddon (1973) and Cleary et al. (1974). Numerical results derived from the theoretical treatment of scattering developed by Haddon (1974) and Haddon and Cleary (1974) are presented and subsequently compared with observational data from the Warramunga (WRA) and NORSAR arrays. The NORSAR data and analysis are described in detail because they have an important bearing on the proper interpretation of the entire teleseismic P coda, and no such detailed results have been previously reported in the literature. The comparison of theoretical and observational results presented, along with other available data, confirm that the precursors to PP ($90^{\circ}<\Delta<110^{\circ}$) are, indeed, likely to originate by scattering of P waves by random inhomogeneities in the crust and uppermost mantle. We remark that since the PP precursors are a major feature of the teleseismic P coda, the results presented herein provide further strong support for the scattering interpretation of the entire P coda.

2 PERSPECTIVE

The "multiplicity of phases recorded between P and PP in the distance range $95^{\circ}<\Delta<111^{\circ}$" were first interpreted by Nguyen-Hai (1963) as being of two types. The first type, whose travel time curve appeared parallel to that of P itself, was interpreted as resulting from top-side reflections from postulated upper mantle discontinuities. This interpretation has subsequently been adopted to explain various coda arrivals by Husebye and Madariaga (1970), Davies and

Frasier (1970), Davies et al. (1971), and Gutowski and Kanasewich (1974); notation of the form pdpP, after Davies et al. (1971) is now widely used to describe the ray paths in question. Nguyen-Hai's second type of coda arrivals were associated with a travel time curve apparently parallel to the PP curve, and were interpreted as resulting from underside reflections at upper mantle discontinuities. Bolt et al. (1968) concluded that the division of the observations into two types was not warranted; they preferred the interpretation in terms of reflections from the undersides of horizontal discontinuities at depth d, say, below the Earth's surface, and adopted the notation P_dP. The travel time data presented by Bolt et al. (1968) and Bolt (1970) is consistent with d being generally less than 400 km.

In subsequent array studies, Wright and Muirhead (1969), Wright (1972) and Angoran and Davies (1972) have shown, however, that the observed precursors generally have slownesses significantly less than the values entailed by the P_dP hypothesis. Wright and Muirhead (1969) and Wright (1972) showed that their observed travel times and slownesses are consistent with an interpretation involving asymmetric reflection from postulated dipping crustal interfaces at distances near 20° from the source. In addition to the lower slownesses, Wright (1972) also observed slownesses significantly greater than those entailed by the P_dP hypothesis, which he showed to be consistent with a similar asymmetric reflection interpretation involving reflection

at distances near 20° from the recording station. Although consistent with the observed times and slownesses, the asymmetric reflection interpretation fails to account for the ubiquity of the precursors, and more importantly the duration and amplitude along observed precursor wave trains. The scattering interpretation will be shown to be consistent with the data in all of these respects.

3. THE SCATTERING INTERPRETATION

The scattering interpretation of the precursors assumes that energy is scattered (i.e., deflected) from ordinary PP ray paths by the presence of relatively small random inhomogeneities in the crust and upper mantle, with normal reflection generally taking place at the Earth's surface (see Fig. 1). The amplitudes of the scattered waves will depend in general on the characteristics of the random medium assumed, the primary wave amplitudes at the points of scattering, the wave frequency, the angular deflections of the scattered wave rays, the volume of the scattering region contributing to the signal at any particular time and the usual focusing and defocusing effects associated with the Earth's velocity structure.

The scattering and asymmetric reflection interpretations are similar insofar as the lower slowness observations are associated with scattering (cf. reflection) of the relatively high amplitude P waves incident at the Earth's surface near 20° from the source (i.e., associated with the so-called "20° discontinuity"). The higher slowness observations

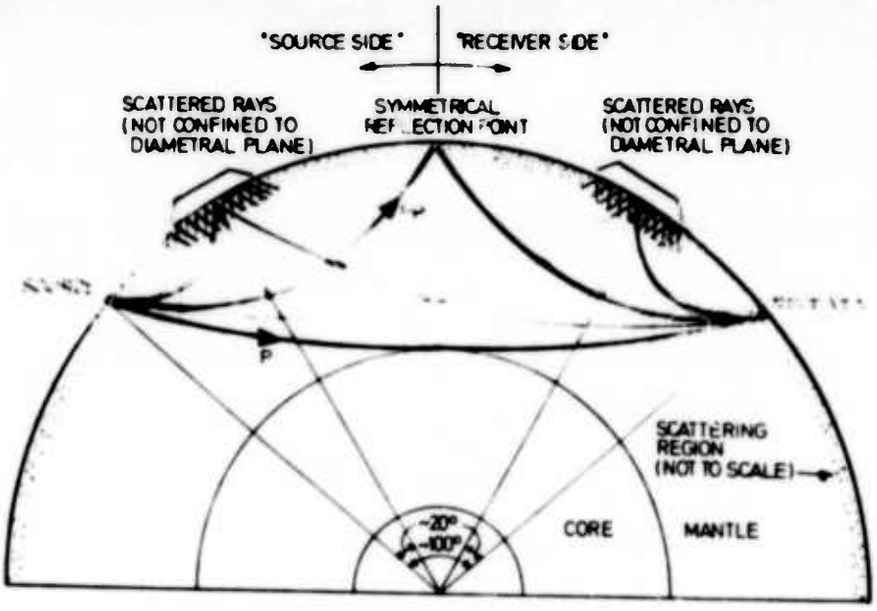

Fig. 1 Schematic diagram showing ray paths of P, PP and precursors to PP resulting from scattering by random inhomogeneities in the crust and upper mantle. The precursor paths are asymmetrical, and are not restricted to the diametral plane through source and receiver.

are associated with conjugate or dual paths in which waves scattered (cf. reflected) at distances near 20° from the receiver tend to be focused towards the receiver by the upper mantle velocity structure. An essential difference between these two interpretations stems from the fact that the scattering process need only involve relatively minor deflections from normal PP ray paths. Such deflections would generally occur at each point of the postulated scattering region and a multiplicity of asymmetric ray paths would generally contribute towards the energy arriving at a receiver at each particular time, the totality of such contributions giving rise to the continuous P coda. The paths would not generally lie in the diametral plane through source and receiver (as represented schematically in Fig. 1). Apparently discrete coda "phases" reported by previous authors consist simply of portions of the coda which are relatively energetic compared with immediately preceding

portions. On the scattering interpretation such circumstances would arise naturally as a random effect, resulting from high constructive interference between scattered wave contributions arriving from different parts of the scattering region, as well as from effects of regional variations in upper mantle structure. Strong evidence indicating the random nature of PP precursors is shown for example in figures 8 and 10 (to be considered in more detail later), where apparently discrete "bursts" of energy on individual traces show little or no correlation with similar bursts on traces recorded on identical seismometers only a few kilometers away. Similar P coda variability across the LASA array has been reported by Davies (1971). In this paper we use the term precursor to refer to the whole of the extended energetic portion of the P coda preceding PP, including any apparently discrete phases which may occur.

Seismic wave scattering in regions of small-scale random heterogeneity in the lowest mantle has been used to explain precursors to the core phase PKIKP ($120^{\circ} \lesssim \Delta \lesssim 143^{\circ}$) by Haddon (1972), Cleary and Haddon (1972), King et al. (1973, 1974) and Haddon and Cleary (1974). In close analogy with the present case, conjugate paths exist for the precursors to PKIKP, and slownesses appropriate to both paths have been observed (Doornbos and Vlaar, 1973; King et al., 1973, 1974).

Scattering within the crust and upper mantle has previously been used to explain the coda of local earthquakes (Aki, 1969; Aki and Chouet, 1974; Dainty and Anderson, 1972)

as well as short-period P wave time and amplitude anomalies at the LASA and NORSAR arrays (Aki, 1973; Capon, 1974; Capon and Berteussen, 1974; Berteussen et al., 1974).

The scattering interpretation of PP precursors completely removes the need for postulating sharp reflecting discontinuities in the uppermost few hundred kilometers of the crust and upper mantle. In this respect, the interpretation differs from studies too numerous to mention. We remark that many of these previous studies have implicitly discriminated against the possibility of scattering type interpretations in their data selection and analysis methods. Indeed, the observational data to be presented serves to illustrate the difficulties likely to be encountered in investigating precursors to PP, or other coda "phases", using data not sampled densely (and simultaneously) in space. As an example, the recent study by Gutowski and Kanasewich (1974) involves data from an array of 5 instruments distributed over an aperture of almost 200 km. The use of such a configuration for studies within the coda is quite unsuitable for the analysis of short period waves having a scattering origin.

4 THE SCATTERING MODEL ASSUMED

The Earth models to be examined are assumed to be spherically symmetrical except for small random variations in density (ρ) and elastic parameters (k, μ) inside the uppermost 100 km of the crust and mantle. Models incorporating the Jeffreys (1939) P and S velocity distributions and a slightly simplified SMAK II model (Mereu et al., 1974)

will be examined, the latter in order to demonstrate the consequences of using a more detailed representation of the upper mantle transition zone. The random variations $\Delta\rho$, Δk and $\Delta\mu$ in ρ, k and μ inside the scattering region are arbitrarily assumed to have root-mean-square values of 1% and to be all proportional to a common stationary random function having a Gaussian autocorrelation function with correlation distance σ=12 km. Such a scattering medium is broadly consistent with the conclusions of Aki (1973) and Capon (1974), who interpreted observed wavefront deviations at LASA in terms of random variations in P velocity having an r.m.s. deviation from the mean of about 2 to 4% down to depths of 60 to 136 km. Comparable results have been obtained from observations of the kinematic and dynamic behavior of P waves at NORSAR by Berteussen et al. (1974).

Under certain simplifying assumptions (see Haddon, 1974; Haddon and Cleary, 1974) the theoretical mean-square amplitudes of first order scattered P waves derived from a simple harmonic primary P wave by inhomogeneities inside a region V of an otherwise spherically symmetrical Earth model are given approximately by

$$\langle\theta^2\rangle = \frac{K}{16\sqrt{\pi}\, r_c^2} \iiint_V \frac{\Gamma^2[E(\alpha_o\tau)]^2 k^4 \sigma^3 \cos e_A \cot e_B}{\eta_B \sin e_B \sin e_C \sin \Delta_{BC}} \left|\frac{d^2T_{BC}}{d\Delta_{BC}^2}\right| \exp(-k^2\sigma^2 \sin^2\phi/2)\, de_A d\psi_B dr_B, \quad (1)$$

where $k = 2\pi/\lambda$ denotes the wavenumber of the primary wave

and all the other symbols are as defined in Haddon and Cleary (1974). In deriving the numerical results, the primary wave envelope function $E(\alpha_o \tau)$ has been assumed to have the simple form

$$E(\alpha_o \tau) = \begin{cases} 0 & \tau < 0 \\ 1 & 0 < \tau < 10 < \text{sec} \\ 0 & \tau > 10 \text{ sec} \end{cases}$$

corresponding to a simple harmonic wavelet of duration 10 seconds. Further details of the scattering theory are given in Haddon and Cleary (1974).

5 THEORETICAL RESULTS

On the random medium hypothesis, scattered waves will generally arrive simultaneously at a receiver R from a wide range of different directions. Fig. 2 shows, for example, the approximate theoretical ranges of slowness and azimuthal direction for scattered waves of PP type arriving at a receiver at an epicentral distance $\Delta = 100^o$ at the times indicated for the Jeffreys velocity model. The scattered wavelets arriving at R at any particular time are seen to consist of two groups, one having slownesses in the range 4.5 to 7.5 sec/deg corresponding to scattering at points nearer to the source than to the receiver, and the other having slownesses in the range 7.5 to 13.5 sec/deg to scattering at points nearer to the receiver than to the source (see Fig. 1). The theoretical slownesses of these two groups will be compared with observational data in a subsequent section.

The two sets of curves in Fig. 2 are conjugate to one another in the sense that scattered wave rays corresponding

to points on any curve in the lower part of the figure are associated with primary wave rays corresponding to points on the curve for the same time in the upper part of the figure and vice versa. It may be noted that the cusps in the curves between slownesses of 4.5 and 5.1 sec/deg in the lower part of the figure are associated with the cusps in the Jeffreys-Bullen P travel time curves near 20°.

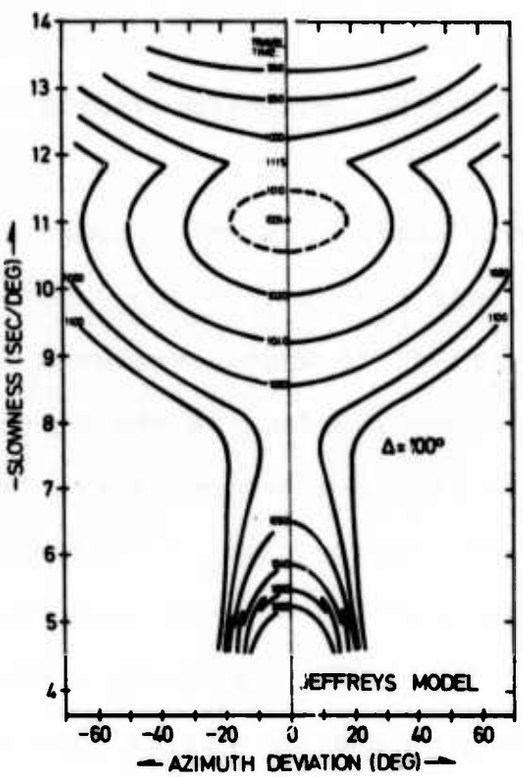

Fig. 2 Ranges of slowness (s/deg) and azimuthal deviation (deg) of waves scattered near the surface of the earth and subsequently arriving at a receiver at $\Delta=100^{\circ}$ at the times indicated for a Jeffreys velocity model. The upper (>7.5 s/deg) and lower (<7.5 s/deg) slowness groups correspond to scattering on the receiver and source sides of the paths respectively. Note the wide azimuthal spread of wave scattered on the receiver side of the symmetrical reflection point.

Fig. 3 shows the corresponding relative theoretical r.m.s. amplitudes of the scattered waves arriving at $\Delta=95^{\circ}$, 100° and 105° for waves of period 1.0, 1.5, 2.0 and 3.0 sec as derived by numerically integrating Eq. (1) for the assumed model. The relative amplitude of the associated direct primary PP arrival as derived using simple ray theory (Bullen Ch. 8) is approximately 2.0 units. It must be emphasized that although the theoretical r.m.s. amplitude curves show smooth amplitude variation, random fluctuations in amplitude along individual wave trains are of course entailed by the scattering mechanism assumed.

The relatively sharp increase in scattered wave amplitudes for $\Delta=105^{\circ}$ near time t=1035 sec shown in Fig. 3 corresponds to the arrival of waves scattered from the relatively high amplitude P waves incident at the Earth's surface at distances near 20° from the source (i.e., from near the so-called 20° discontinuity) and from waves following conjugate paths where scattering takes place about 20° from the receiver. Following the amplitude increases from t=1035 sec to about 1050 sec, the theoretical r.m.s. scattered wave amplitudes remain moderately large right up until the arrival time of the main PP phase. Similar comments apply to the results for the other two distances given. The results given have been obtained assuming a surface focus; the results would not, however, be expected to be significantly different for focal depths of up to 100 km or so. For much deeper foci the results may differ significantly, because for foci at depths >413 km in the Jeffreys

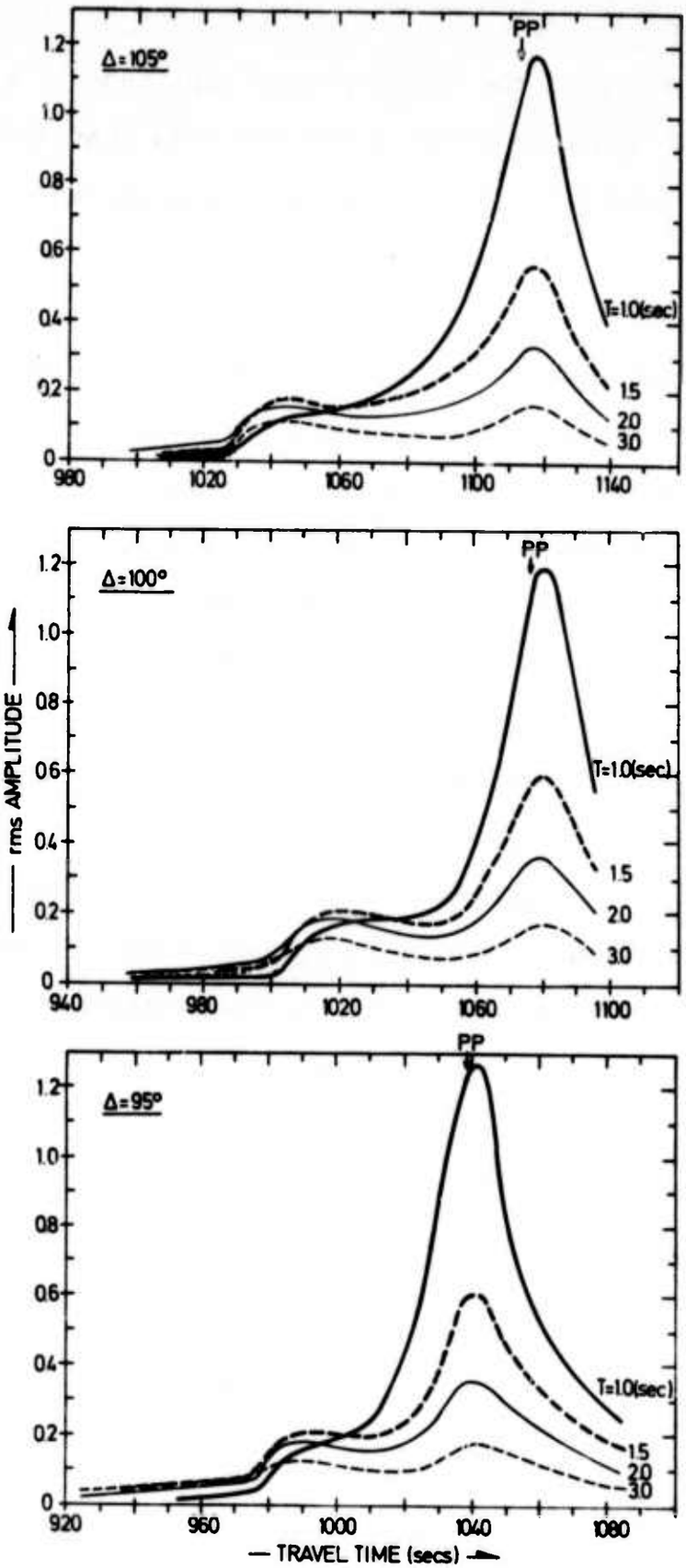

Fig. 3 Theoretical r.m.s. amplitude variations along scattered wave trains at $\Delta=95^{\circ}$, 100° and 105° for the Jeffreys velocity model and simple harmonic primary wave trains of period 1.0, 1.5, 2.0 and 3.0 secs and 10 sec duration. The associated amplitude of the primary PP phase as derived using simple ray theory, is 2.0 units.

model, for example, the primary wave amplitude at the surface of the model would be quite different from that for a surface focus, since the T-Δ curve is single-valued in the former case.

The effects on the theoretical results of replacing the Jeffreys upper mantle velocity distribution by a substantially different upper mantle distribution as represented, for example, by a slightly simplified version of the SMAK II model of Mereu et al. (1974) are now examined, since it is now known that the velocity gradients in the upper mantle transition zone can differ significantly from those in the Jeffreys distribution. The Jeffreys and the simplified SMAK II velocity distribution used in the calculations are plotted for comparison in Fig. 4. The amplitude and (s,↕) calculations involved in Figures 2 and 3 were repeated for the SMAK model, and the corresponding results are presented as Figures 5 and 6.

An important difference between the results for the two models arises from the shift of some 4° to shorter distance of the caustic point C associated with the "400 km discontinuity" in the SMAK model (see Fig. 4) due mainly to the shallower depth (315 km) of this discontinuity as compared to the Jeffreys model. This results in the build-up of amplitude in the theoretical precursor wave trains occurring up to about 20 seconds earlier for the SMAK model than for the Jeffreys model (cf. Figs. 3 and 6). Another important difference (cf. Figs. 2 and 5) is that in place

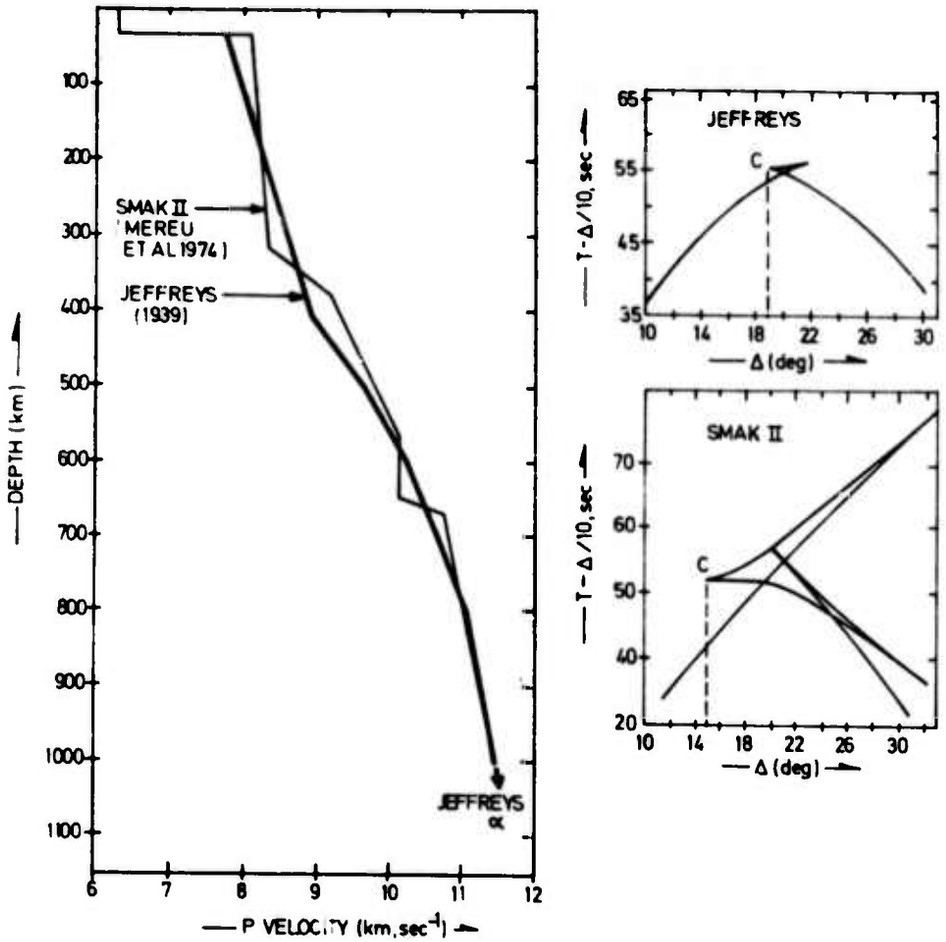

Fig. 4 Comparison of the Jeffreys (heavy line) and a slightly simplified SMAK II (lighter line) upper mantle P velocity models used in theoretical calculations. Note that the caustic cusps C in the associated reduced travel time diagrams occur near $\Delta=19^{\circ}$ for the Jeffreys model but near $\Delta=15^{\circ}$ for the SMAK II model.

of the single group of higher slowness scattered wave arrivals for the Jeffreys model there are two distinct groups in the SMAK II model, corresponding to the two sets of T-Δ branches associated with the abrupt changes in velocity gradient near 315 and 670 km in the latter (Fig. 4). The differences between the (s,Φ) results shown serve to indicate the extent to which regional variations in upper mantle structure may affect the slownesses and azimuths of scattered wave arrivals. In particular, the differences indicate that the uncertain-

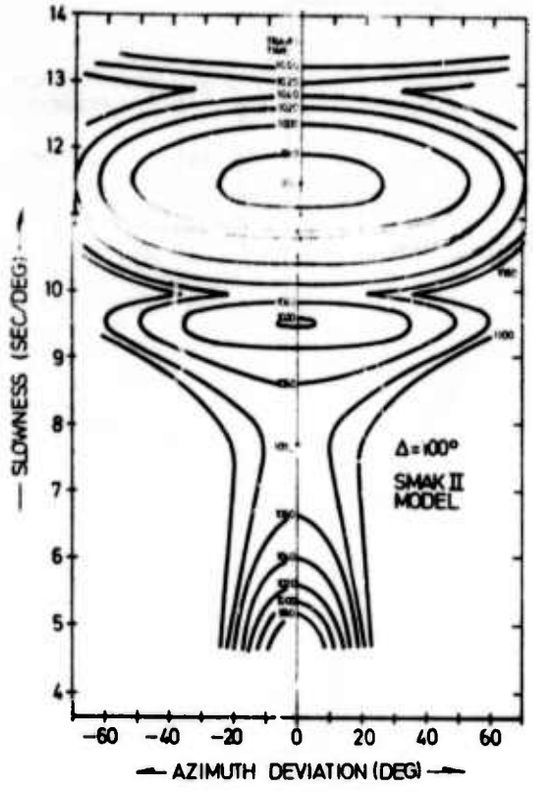

Fig. 5 Ranges of slowness and azimuthal deviation of waves scattered near the surface of the earth and subsequently arriving at a receiver at $\Delta=100^{\circ}$ at the times indicated for the SMAK II model (cf. Fig. 2). Note that for the SMAK II model there are two subgroups of higher slowness arrivals corresponding to the two sets of T-Δ branches for this model shown in Fig. 4.

ties do not warrant a very precise interpretation of slowness observations in the higher slowness range (>7.5 sec/deg), as will become apparent later. The theoretical results given here will be compared with observational data in a subsequent section.

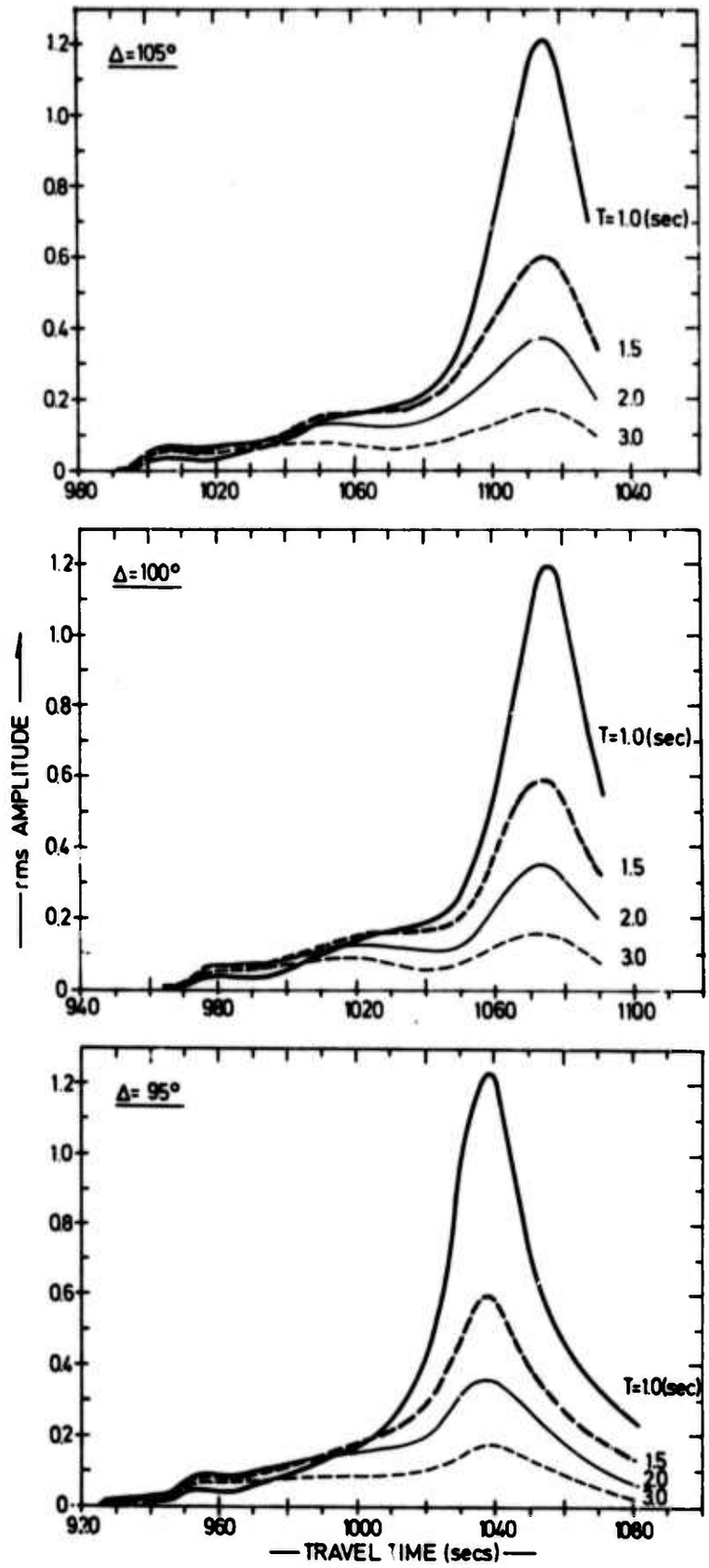

Fig. 6 Theoretical r.m.s. amplitude variations along scattered wave trains for $\Delta=95^{\circ}$, 100° and 105° for the SMAK II velocity model (cf. Fig. 3).

6. DATA AND ANALYSIS

The analysis techniques used in the compilation of observational data suitable for a meaningful comparison with theoretical results are crucially important in the present context, and so will be described in detail below. Since the analysis of the WRA data to be examined has been discussed elsewhere (Cleary et al., 1974), the present section will be confined to the selection and analysis of NORSAR data.

6.1 Data Selection

The phenomenon under examination manifests itself over many seconds and wide (s,Φ) ranges (e.g., see Figures 2 and 5). It is essential that for each event examined, the processing "space" is of comparable dimensions and is sampled in adequate detail. These requirements present us with a computational problem of unusual magnitude, and so we have restricted attention to 3 events. Since the full-aperture NORSAR array began to operate on a routine basis in 1971, events of suitable magnitude and in a suitable distance range for analysis ($m_m > 5.6$, $90^\circ < \Delta < 110^\circ$) have occurred in the two distinct source regions framed in Fig. 7. One event in the Northern Chile region (in region A, Fig. 7) and two events from the Molucca Passage (in region B, Fig. 7) were selected for analysis, the hypocentral information for which is listed in Table 1. These events allow us to examine in detail precursor wave trains from two widely separated source regions, and also to make comparisons between data from within a relatively

Event No.	Date	Origin Time	Lat	Long	m_b	Depth	Distance (NORSAR)	Azimuth (NORSAR)	Region
1	Jan 02 1974	10 42 29.9	22.5S	68.4W	6.0	105	104.3	249.6	N. Chile
2	Mar 16 1973	00 51 47.0	2.1N	126.6E	6.0	18	100.5	66.2	Molucca Passage
3	May 11 1974	00 43 44.9	1.7N	126.4E	6.0	N	100.7	66.6	Molucca Passage

TABLE 1

Hypocentral information for NORSAR events analysed.

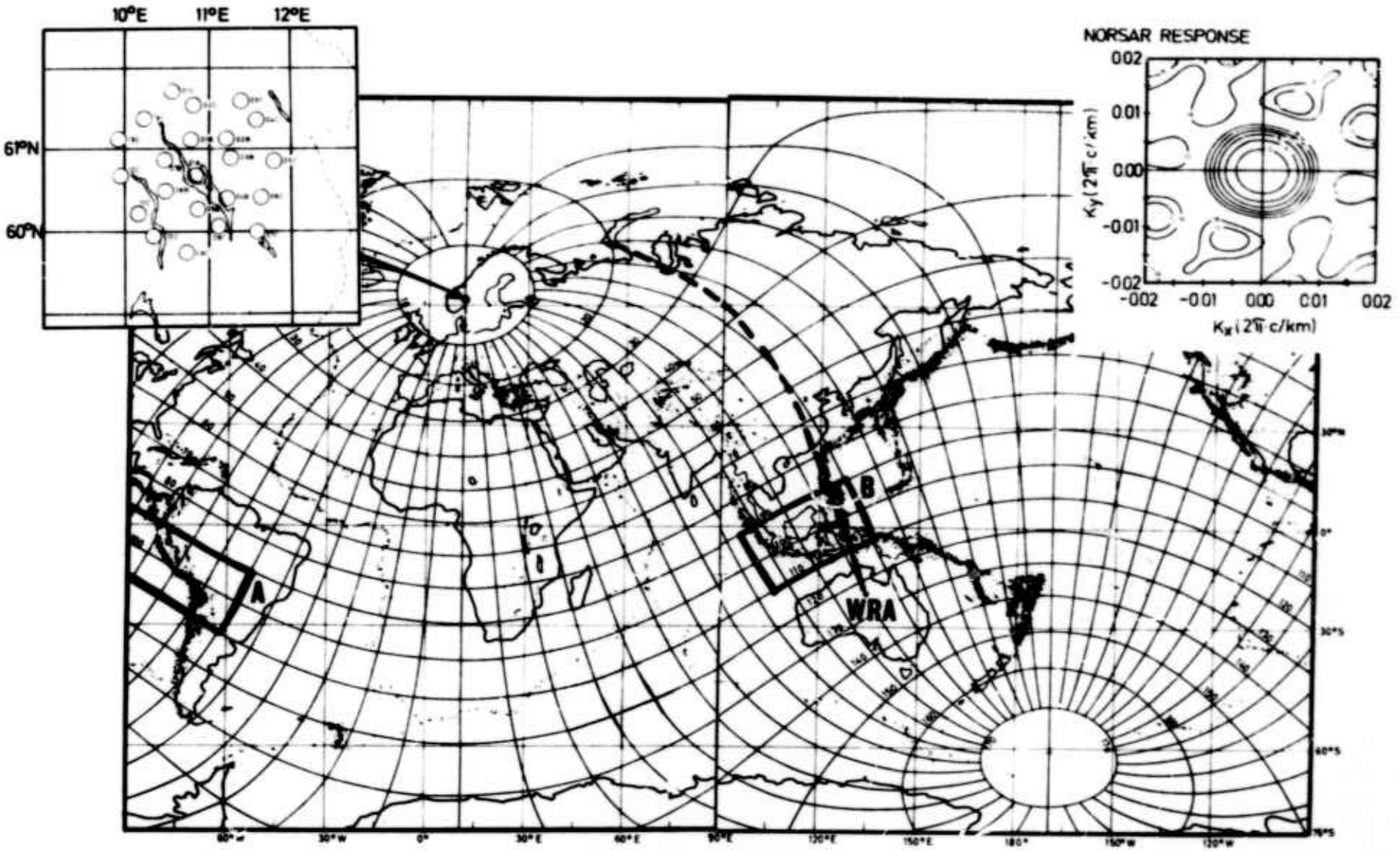

Fig 7. Caption at bottom of following page

before PP than have some channels with much lower P amplitudes (02B, 03B). The small power level variations, as well as the extended duration of the PP precursor wave train, suggests immediately that the precursor generating mechanism is effective over a large region of the Earth's upper mantle, (i.e., a large area of slowness-azimuth space). All these features, as well as the arrival time of the energy relative to the P arrival time, cannot be satisfactorily explained by structural complexities in the immediate vicinity of NORSAR, but are fully consistent with the expectations of the scattering interpretation. Also consistent with theoretical expectations (briefly referred to in an earlier section) is the relative lack of coherence between even closely separated subarrays (see NORSAR configuration, inset in Fig. 7). In fact the recordings from the 6 instruments within individual 7-km subarrays, such as those plotted in Fig. 9, display only quasi-coherence, and are suggestive of extensive interference between a plethora of arrivals arriving from different directions. Note that the traces in Fig. 9 are each normalized independently, and have been filtered in the frequency range 0.6 Hz to 3.0 Hz.

Fig. 10 is comprised of selected data from subarray central instruments for events 1 and 2 (Table 1). In the time interval of particular interest (i.e., two or so minutes preceding PP), although the traces in this figure differ in detail both within the array aperture for a single event and also between the separate events, all of the data presented appears to exhibit the same general character.

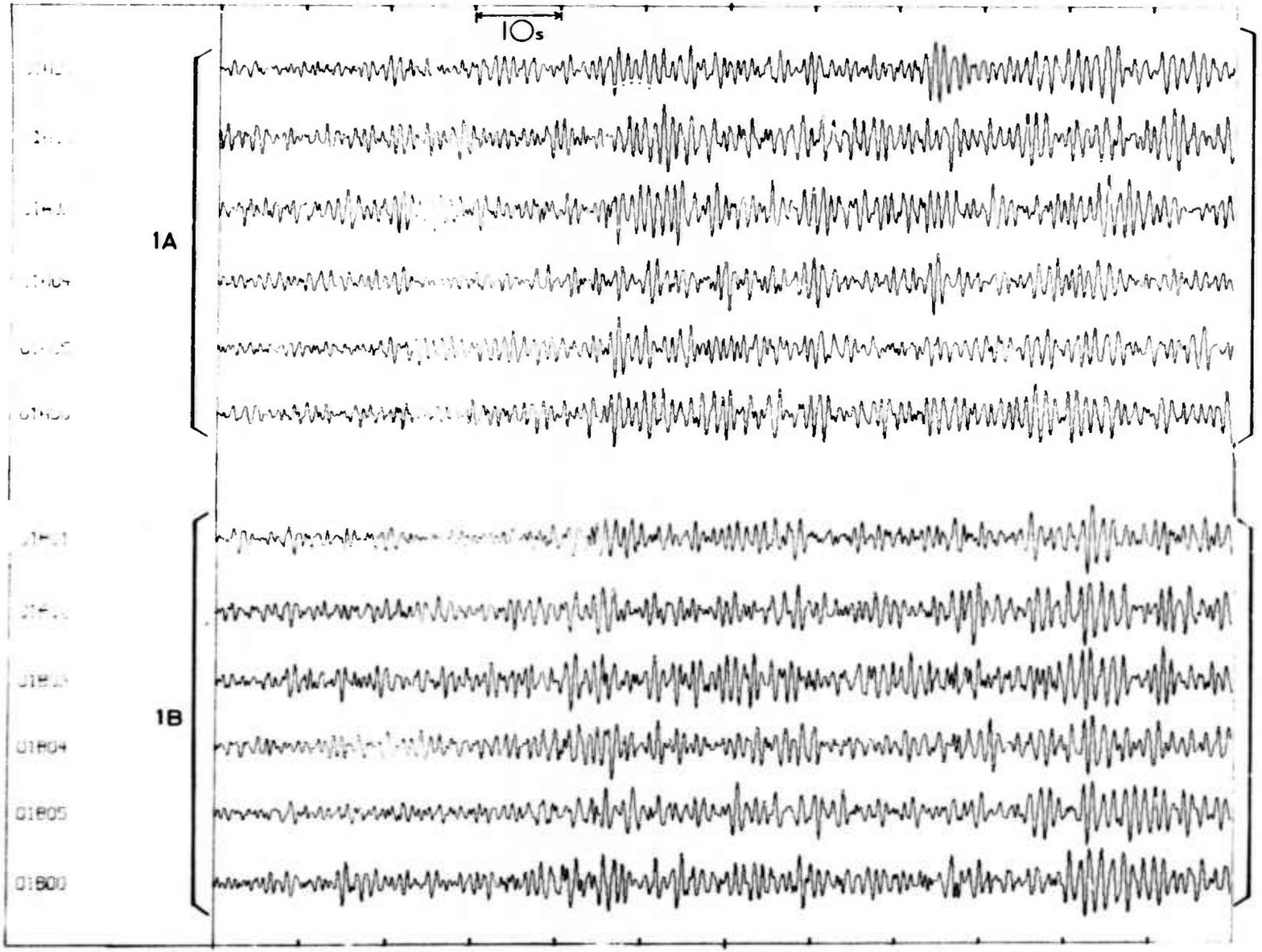

Fig 9. Caption at bottom of following page.

We will demonstrate shortly, however, than in respect of the (s,Φ) structure, the data from the two different regions are very different. Fig. 10 includes one trace (labelled LG) plotted more as it might appear on the recording from a conventional "analogue" station. This particular trace is dominated by the strong core phase arrival (PKiKP), and the details of the coda and PP itself are lost. This example serves to illustrate the importance in studies of this kind of having magnetically recorded data and the associated capability to increase arbitrarily the gain in plotting.

6.2 Data Analysis

The processing procedure adopted for investigation of the distribution of power in time, slowness and azimuth involved the formation of some 588 array beams for each second of data analysed. The search space adopted was 4 to 12 sec/deg for slowness and $\Phi_{expected} \pm 60^{o}$ for azimuth, although the slowness range 12 to 15 sec/deg was also investigated on an exploratory basis for selected time intervals. Intra-subarray time delays were calculated and subarray beams formed for 12 (s,Φ) "reference" directions distributed symmetrically within this search space by summing the 6 appropriately phased traces for each of the 22 subarrays. Using the subarray beams for each reference direction in turn the inter-subarray delays were varied as appropriate for direc-

Fig. 9 Precursor section of seismograms from all 6 of the short period instruments of the 7-km aperture subarrays 01A and 01B for event 3. The plot start time is 1 hr 0 mins. Each of the traces shown has been filtered in the range 0.6 Hz to 3.0 Hz and normalized independently of the others.

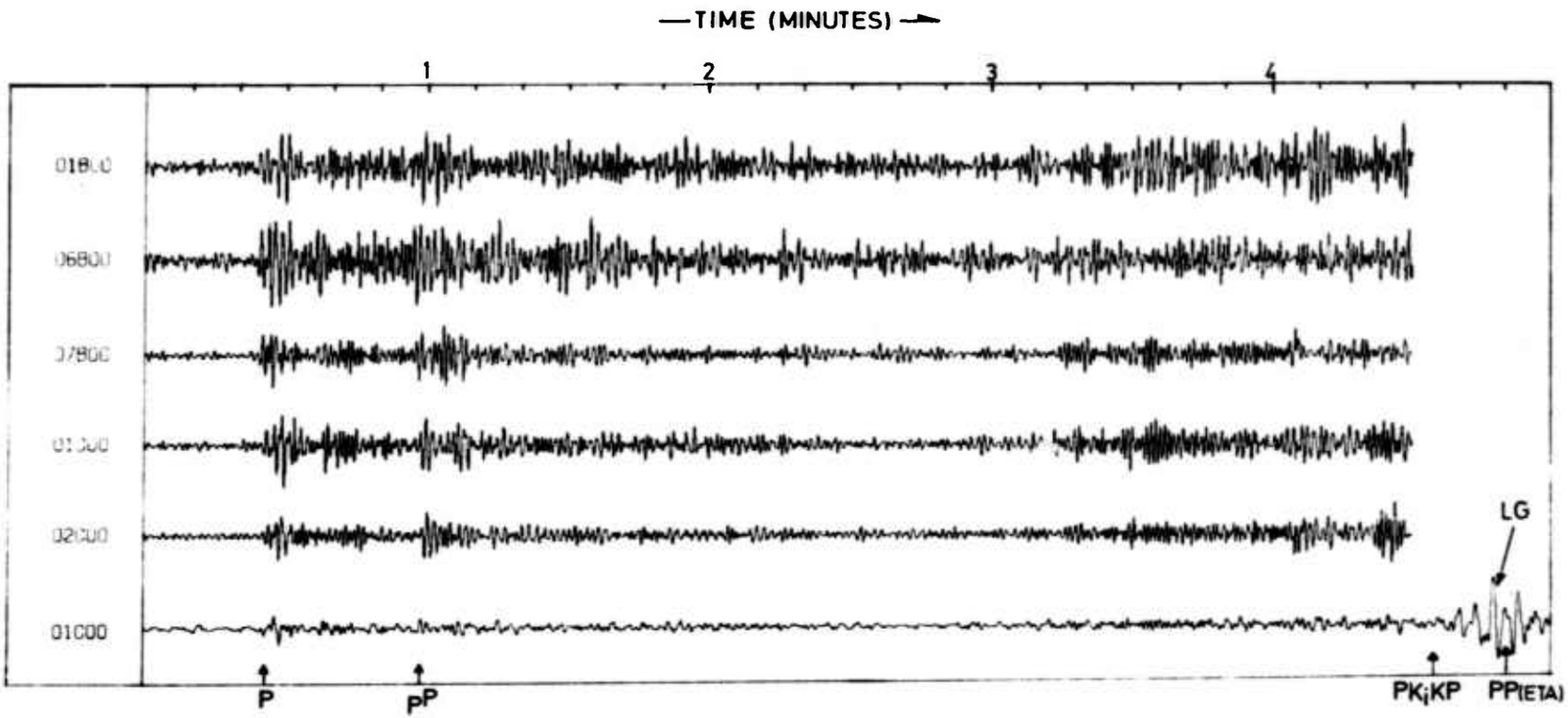

Fig. 10a Seismograms from 6 selected subarray central instruments (as labelled) for event 1. The uppermost 5 traces have been filtered in the range 0.6 Hz to 3.0 Hz. The data start time is 10 hrs 56 mins. The uppermost 5 traces have been terminated before the arrival of PKIKP in order to show details of the PP precursor wave train. In the bottom trace, labelled LG, the data from subarray 01C has been plotted with PKiKP (and PP) included. This trace shows how details of PP precursor arrivals might be lost at a conventional "analogue" seismograph station.

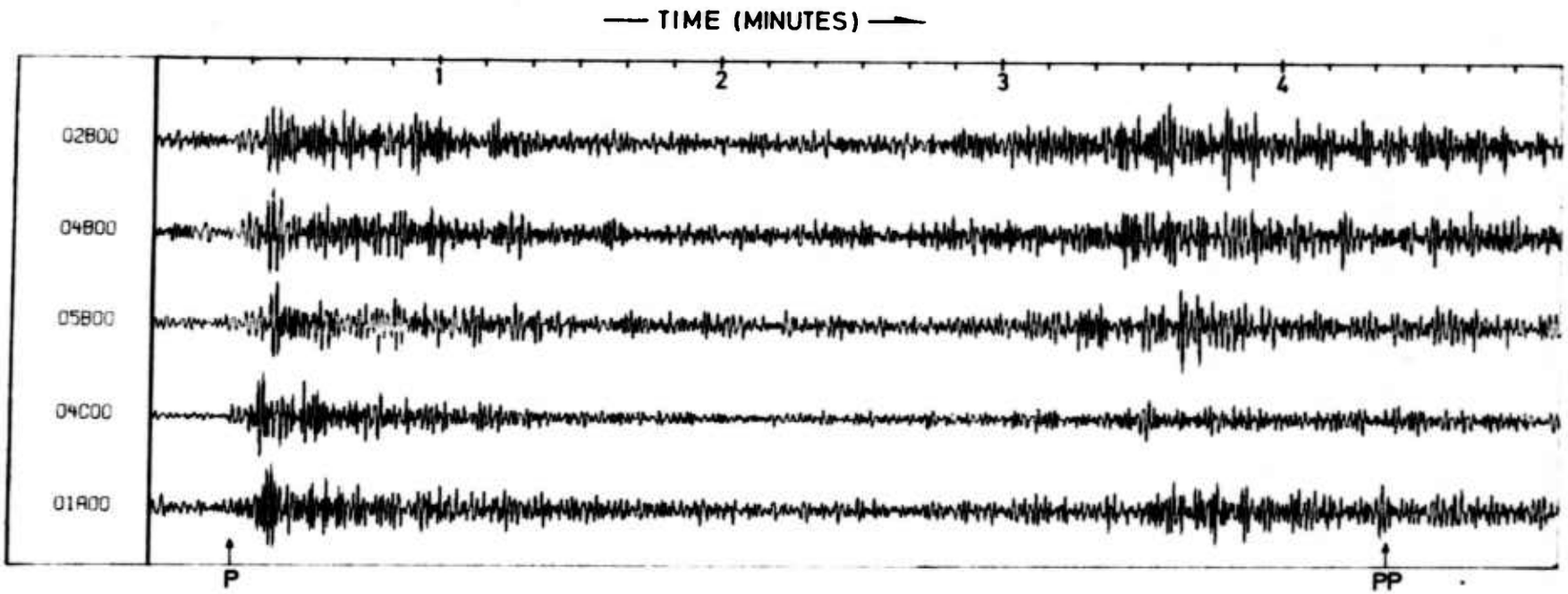

Fig. 10b Seismograms from 5 selected subarray central instruments (as labelled) for event 2. The traces shown have been filtered in the range 0.6 Hz to 3.0 Hz. The plot start time is 01 hrs 05 mins.

tions corresponding to each point in turn of a symmetrical grid of 7 x 7 (s,Φ) values centred on each reference direction. The beam "power" (energy per second) was evaluated for each grid point by summing the phased subarray beams to form a full array beam, and then summing squared full array beam amplitudes over 20 samples (1 second). This procedure yielded beam power at each point of a 14 x 42 grid, with spacing 0.62 sec/deg and 3.1° in s and Φ respectively for each second of data analysed. With regard to systematic errors in the (s,Φ) values, the time delays appropriate to the (s,Φ) values defining the grid points were "decalibrated" in the processing using the NORSAR empirical time delay correction base (Berteussen, 1974). Since this correction base is near optimal, the decalibration procedure should effectively remove any serious distortion in the grid point locations arising from structure underlying NORSAR.

The processing procedure described was used to process the 105 consecutive seconds of events 2 and 3 immediately preceding and including the PP arrival, and the 120 seconds of event 1 preceding the PKiKP arrival. In addition, a five second noise sample preceding P, P itself and some 85 seconds of the "early" coda of event 3 were also analysed for comparison with the precursor section of coda. Since a single 15 second data interval required a minimum of 90 minutes processing time on the IBM 360/40 computers at the NORSAR Data Processing Center, the enormity of the computation problem requires no further emphasis. Alternative processing procedures were, of course, considered, but lacked sufficient robustness in the complex signal situation at hand.

The values of power at each (s,Φ) grid point for each second of the wave train were outputed on cards or magnetic tape for subsequent contouring in a separate processing step. In order to facilitate the interpretation of power peaks for subsequent comparison with theoretical results such as those presented in Fig. 2, contour plotting in the slowness-azimuth plane of power value averaged over 2 or 3 seconds was found to be most suitable for digestion of all results. A typical slowness-azimuth power plot for a 3 second data segment of total travel time 1025 secs (Event 2) is illustrated in Fig. 11. Vespa-type plots (Davies et al., 1971) in the diametral azimuth, but with some control exercised over the array azimuthal response by incorporating data from adjacent azimuth-time planes in an averaging procedure, were also plotted (see Fig. 16).

6.3 Interpretation of Slowness-Azimuth Diagrams

The processing described effectively transforms the array data into a convenient representation in slowness-azimuth space by the application of a family of matched spatial filters. It is essential to give consideration to the response of these filters in slowness, azimuth and time in order that any information extracted from the transformed data can be reliably ascribed as a "true" manifestation of Earth structure rather than as an artefact of the processing. We are concerned in particular with establishing criteria for assigning significance to the various peaks in the contour plots of power in the slowness-azimuth planes (e.g., Fig. 11).

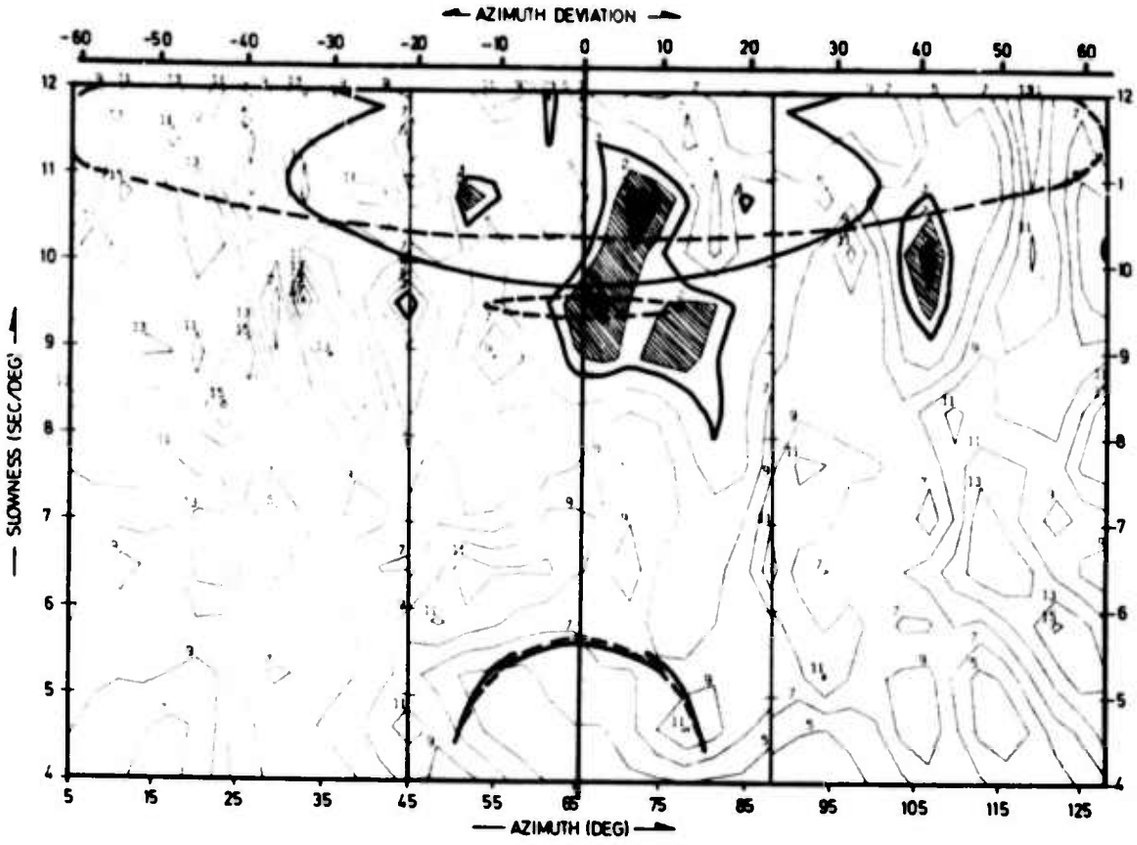

Fig. 11 Contoured beam power levels in slowness-azimuth space averaged over 3 seconds for a mean travel time of 1025 sec for event 2. The contours represent power levels in dB below the absolute maximum. The 3 dB contour is darkened, and regimes of power levels between 2 and 1 dB and 1 and 0 dB are hatched and dotted respectively. Theoretical slowness-azimuth curves for scattered wave arrivals for a travel time of 1025 sec and for $\Delta=100^{\circ}$ for both the Jeffreys (solid line) and SMAK II (broken line) are plotted for comparison with the observed power distribution. Note that the locations of the maximum power peaks shown are in close agreement with the theoretical curves. Also note the wide spread of azimuths of observed power peaks in this example. This spread has been frequently observed in the present study for the higher (but not the lower) slowness group of arrivals (cf. Figs. 13, 15 and 18).

The beamforming response of the NORSAR array to a monochromatic steady-state signal has been discussed by several authors and is conveniently represented in wavenumber space (see inset to Fig. 7). The response to broadband transient signals is a smoothed version of the steady-state response (Kelly, 1967; Steinberg, 1971), but can differ also in the mean sidelobe level (see Steinberg, 1971). In a typical case observed at NORSAR, the worst sidelobe in the response of a beam power analysis on the main P signal from Event 2 (Table 1) was measured to be slightly less than 10 dB below the main lobe level; this is some 5 dB worse than the level indicated by the steady-state theory. Such discrepancies are probably due mainly to the variations in signal amplitude and shape within the array aperture, which violate certain fundamental assumptions in the steady-state calculations. Indeed, Doornbos and Husebye (1972) have demonstrated that amplitude variations between individual sensors can have the effect of introducing spurious side lobe peaks into the array response. Such effects are expected to be troublesome in the analysis of PP precursor wave trains insofar as the individual contributions to the wave train are subjected to similar distortions as the main P signal by structure beneath the array.

The response of the array to a composite signal, involving several interfering contributions of various amplitudes and arrival directions, cannot be simply estimated from a superposition of appropriate steady-state responses and is extremely complex. In addition, the time response

of the array, which depends on the duration and pulse shape of a transient arrival, will act to restrict the resolution of interfering components. Doornbos and Husebye (1972) investigated some of these effects using synthetic data and elucidated the difficulties in interpreting array beam information in the presence of multiple arrivals. In slowness-azimuth space the situation is further complicated by the fact that the response pattern for each arrival separately depends on the particular arrival direction.

In view of these difficulties, we examined our data directly in order to establish empirically an "interpretation threshold" in the contoured power plots of 2 to 3 second data intervals. This examination revealed that interpretation of power peaks more than 2 to 3 dB below the most energetic power peak would be problematic in that it would greatly increase the number of peaks per time interval. In view of the array time response limitations, it seems unreasonable to extract multiple peaks within a 2 to 3 second interval, except perhaps in the situation where peaks of very similar power are present, and so this threshold is a purely practical one. We remark that if we chose to interpret all peaks down to 6 dB, say, many of the measured values would then find no explanation in the scattering or any other suggested interpretation. However, at this level all the "spurious" peaks, without exception, occur in time intervals containing a more powerful "valid" peak, which suggests that the numerous peaks 3 to 6 dB below the main peak are likely to be artefacts of the array response in an extremely complex signal situation.

It is relevant to comment on the distinction between our interpretation threshold as compared to that suggested by Capon and Davies (1971), who investigated the specific problem of interpreting contoured beam power diagrams produced with a processor similar to that used in the present study. These authors utilized techniques of statistical pattern recognition in establishing criteria for detecting significant arrivals (i.e., power peaks) within a signal-generated coda, and concluded that a "discrete seismic arrival" could be declared present for a minimum contrast of 9 dB between the main peak power and the average background noise level just prior to signal arrival. Although these authors used this criterion to examine arrivals within the teleseismic P coda, we differ insofar as their assumed threshold is based on the distinction between so-called signal and supposedly independent preceding noise. Such a distinction is inappropriate in the present investigation in which we are seeking to determine approach directions of contributions having relatively high intensity within wave trains which consist of sums of contributions of similar intensities arriving from widely different directions (cf. Figs. 2 and 5). In such circumstances all the contributions arriving from directions within the main lobe of the array response pattern appropriate to a particular direction may be thought of as constituting the "signal" corresponding to that direction. All contributions not encompassed by the main response lobe then effectively constitute the "noise". Since the main response lobe corresponds to a range of directions much smaller than the total range of directions from which the various contribu-

tions could arrive (cf. Figs. 2 and 5), the "signal-to-noise ratio" is likely to be generally poor and so well-defined high intensity peaks would not be expected. It is to be expected, however, that absolute maximum energy peaks obtained in a search of the entire (s,Φ) space would usually correspond to directions of relatively high scattered wave intensity, although exceptions may sometimes occur because of some of the effects discussed above.

In summary, beam power values have been evaluated at each point of an extensive grid of (s,Φ) values for each of many consecutive seconds of data from three events. These data have subsequently been combined over 2 and sometimes 3 seconds, and power values contoured in the slowness-azimuth plane. The largest power values in continguous 15 second time intervals were used as reference levels in the appropriate consecutive plots. The slowness and azimuth values corresponding to no more than two significant peaks in each contour plot were recorded and will be compared with the theoretical expectations of the scattering interpretations in the following section.

7. COMPARISON OF OBSERVATIONS WITH THEORY

In this section, observational data from the WRA and NORSAR arrays will be compared with appropriate theoretical results. We have chosen to use theoretical amplitude results for σ=12 km, T=3.0 secs (cf. Figs. 3 and 6) for comparison with observed amplitude variations despite the fact that the dominant periods in the observational data are significantly less than 3 secs (~0.3-1.7 secs). We

do not consider this apparent mis-match to be serious, however, because the relative amplitudes of the observed PP precursors are much too large for the linear scattering theory to be strictly applicable. Indeed, the dominance of precursor (scattered) energy over direct PP energy in our observational data (see Figs. 8, 10, 12) indicates that scattering effects are so strong that there can be no distinction between primary and scattered waves. In these circumstances results from the linear theory may still be used to model consequences of the postulated scattering process, but the parameters σ and T do not then have their usual physical significance; the applicability of linear scattering theory in such circumstances is discussed more fully in a later section.

7.1 Observations at Warramunga

Fig. 12 shows processed traces of two Novaya Zemlya explosions recorded at WRA ($\Delta=106^{\circ}$) on October 27th, 1966, and October 14th, 1970, compared with corresponding theoretical r.m.s. amplitude curves for scattered waves derived for a Jeffreys model and a period of 3.0 seconds. Note that i) the amplitudes of the observed PP precursor wave trains start to increase to relatively significant values about 85 secs before the arrival of the main PP phase, and ii) the observed amplitudes remain significant right up until the arrival of PP. In both of these respects the observational data are in good agreement with the theoretical amplitude variation curves.

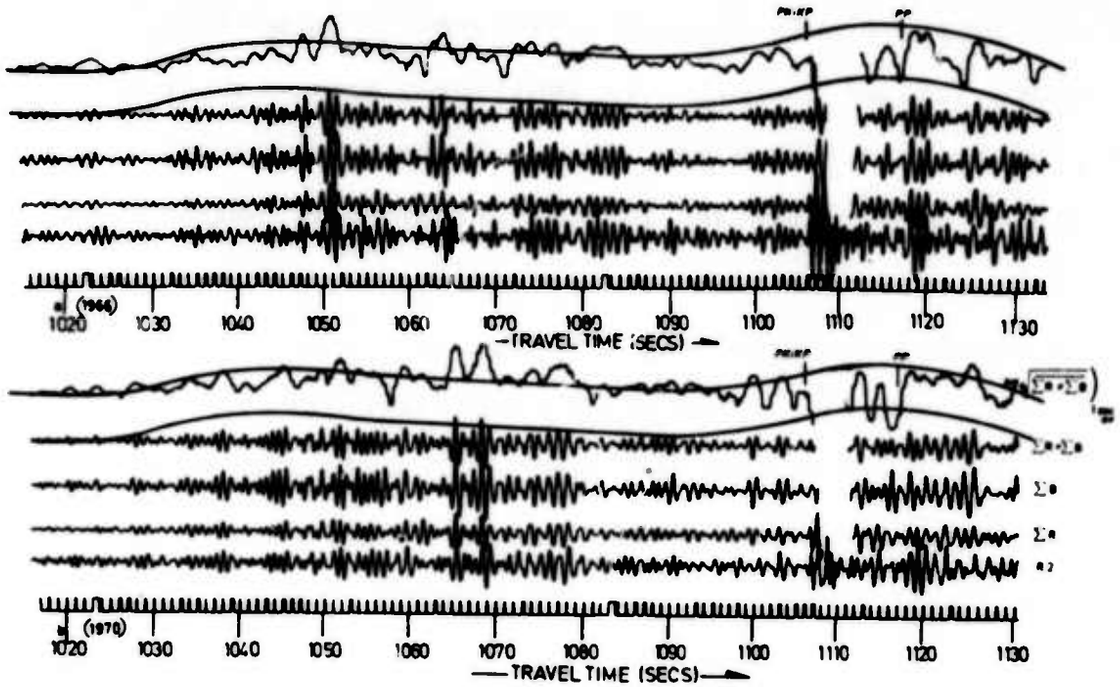

Fig. 12 Processsed WRA array traces showing PKiKP, PP and precursors to PP from Novaya Zemlya explosions (Δ=106°) on 27 October 1966 (example (a)) and 14 October 1970 (example (b)). The traces shown are (from bottom) time channel, single seismometer output, delayed summation of both red and blue line seismometers ($\Sigma R, \Sigma B$), array beam ($\Sigma R+\Sigma B$) and one-second time averaged product (SIG $\sqrt{(\Sigma R \times \Sigma B)}$). Sections (a) and (b) have been aligned according to travel time. Note the duration of the precursor wave trains, and also the marked difference in the arrival time of precursor energy maxima from two explosions which had almost identical location (Δ=106°). Theoretical r.m.s. amplitudes for Δ=105°, T=3.0 sec, for the Jeffreys velocity model are plotted for comparison with the data.

Comparison of the two observed wave trains shown in Fig. 12 also provides clear evidence of the random nature of precursor wave trains, as was originally pointed out by Cleary et al. (1974). The notable dissimilarities in the wave trains from two sources in a similar location are extremely difficult to account for on any previously suggested interpretation of the precursors, but are fully consistent with the random variations to be expected with the scattering mechanism when the source locations are separated by a distance comparable with or larger than the characteristic size of the inhomogeneities present.

Cleary et al. (1974) have shown that the slowness of the precursor wave train for the 1970 explosion migrates to higher values with increasing time. The corrected slowness values (see Cleary et al., 1974) for the signals some 80 and 40 seconds before the PP arrival are plotted on the appropriate theoretical slowness-azimuth diagram in Fig. 13. Also plotted on this figure are some results for an event at a distance of 105.5° from the Yellowknife array presented by Wright (1972), these results representing the first reported precursor slownesses significantly higher than the PP slowness. The agreement between observed and theoretical results in Fig. 13 is fully satisfactory in all cases.

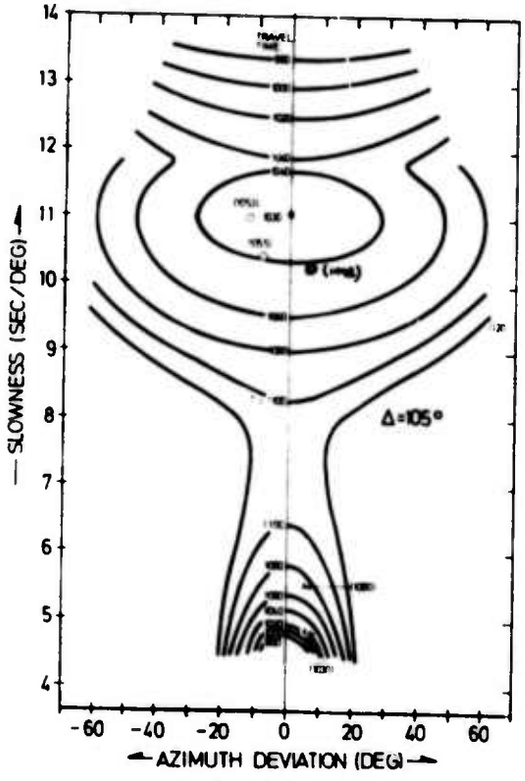

Fig. 13 Measured WRA (s,Φ) values (crosses) for the 14 October 1970 wavetrain (example (b), Fig. 12) compared with theoretical (s,Φ) results for Δ=105° for the Jeffreys model. The measured slowness values are labelled with their corresponding measured travel times. Also shown (dots in circles) are some slowness measurements made at the Yellowknife array by Wright (1972) for his event 11.

7.2 Observations at NORSAR

Event 1

Six subarray central instrument traces and their corresponding short-term-average (STA) traces, obtained by simple rectification and smoothing, are plotted in comparison with the theoretical r.m.s. amplitude curves for both the Jeffreys and SMAK models in Fig. 14. The theoretical curves correspond well with the general features of the observational data. No comparison with the PP arrival is possible as a result of the strong PKiKP arrival (see Fig. 10). The observed travel times in Fig. 14 have been corrected for focal depth (~105 km) by the addition of 15 seconds, which is half the measured P-pP separation (see Fig. 10a). The slowness-azimuth measurements corresponding to the corrected travel times are plotted in Fig. 15. The high slowness range of the theoretical results has been excluded since no significant energy peaks having slownesses in this range were found. The grouping of measurements into 20 second time windows reflects the fact that a more precise interpretation is not warranted.

Scrutiny of Fig. 15 shows that the (s,Φ) data is in satisfactory agreement with the theoretical results. In particular, the small observed deviations from "true" azimuth correlate well with the lower slowness values observed; this effect is remarkably consistent with theoretical expectations as indicated by the concave downward curvature of the (s,Φ) curves for the lower slowness group in Fig. 2. Since all measured slownesses are within $\pm$ 15° of the diametral azimuth, the observational data can be conveniently

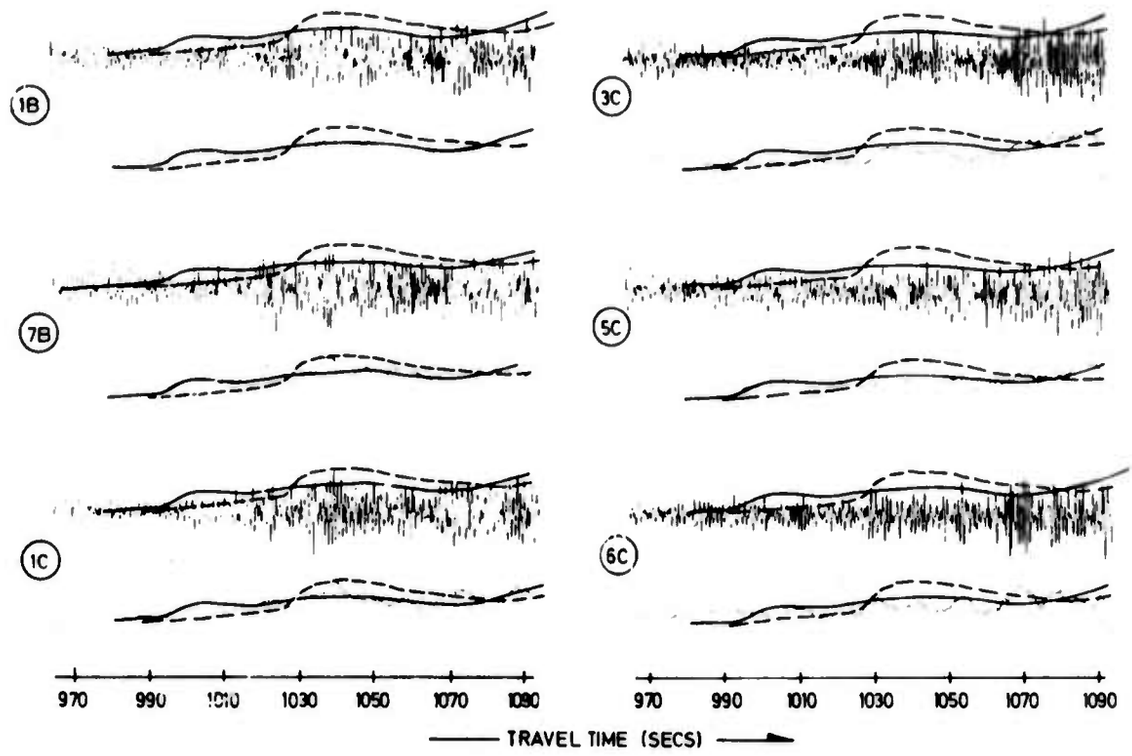

Fig. 14 Seismogram traces (filtered in the range 0.6 to 3.0 Hz) and associated short term average (STA) traces, showing PP precursor wave train at 6 selected NORSAR sub-array central instruments (as labelled) for event 1 in comparison with relative theoretical r.m.s. amplitudes for the Jeffreys (broken line) and SMAK II (full line) models for $\Delta=100^{\circ}$ and T=3.0 secs (see Figs. 3 and 6). The amplitude scale for the theoretical results has been chosen arbitrarily for satisfactory correspondence with observed amplitudes, but is the same in all parts of the figure.

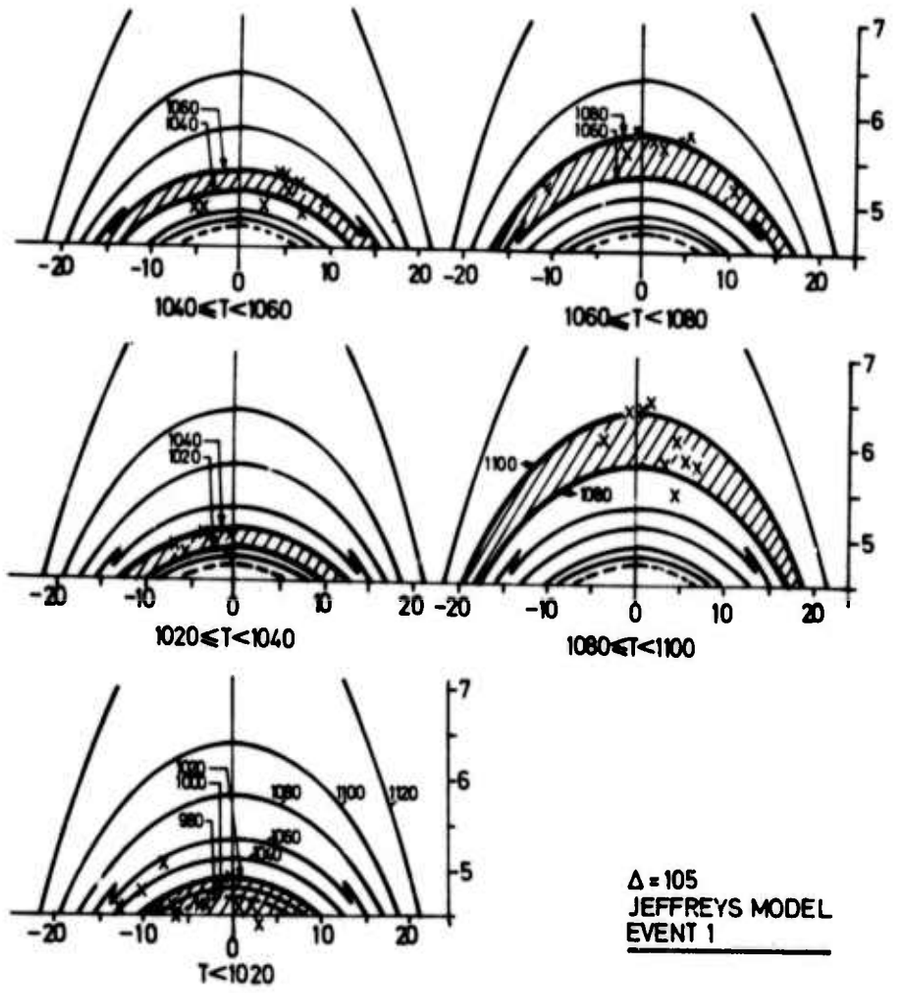

Fig. 15 Measured (s,Φ) values at NORSAR for event 1 plotted in comparison with theoretical (s,Φ) values for $\Delta=105^{o}$ for the Jeffreys velocity model. The higher slowness range (cf. Fig. 2) has been omitted since no significant power peaks were detected in this range. The measured values are grouped in depth-corrected travel time intervals of 20 secs as labelled, and the theoretical (s,Φ) distributions corresponding to each of these time intervals are hatched on the appropriate part of the figure.

summarized in a Vespa-type plot. Such a plot is presented as Fig. 16, but this plot differs from a conventional Vespagram insofar as the data from 6 adjacent azimuth ranges has been averaged in the calculation of the power values. The migration of values to higher slowness with increasing time is clear. The bounds of the lower slowness group in the theoretical results included in Fig. 15 are superimposed on Fig. 16 to facilitate comparison. The power values at slownesses >8 sec/deg are almost exclusively 8 dB or more below the peak powers at lower slownesses.

Events in Region B

In Fig. 17 the theoretical r.m.s. amplitudes for both the Jeffreys and SMAK models are compared with the frequency filtered and STA traces from 6 subarray central instruments for each of Events 2 (Fig. 17a) and 3 (Fig. 17b). The observational data agrees satisfactorily with both theoretical curves, although the gradual energy build up after about 970 seconds is perhaps in better agreement with the results derived for the SMAK model.

The measured (s,Φ) values for both of these events are plotted on theoretical curves for the SMAK model in Fig. 18a to e. The SMAK model is preferred for this comparison since it proved marginally superior in explaining the observational data. Both models accomodate the observational data reasonably well, however, and a discrimination between various upper mantle velocity distributions on the basis of our data is not really justified. In all, 76 data points are plotted in Fig. 18; more than one half of these are in complete agreement with theoretical expecta-

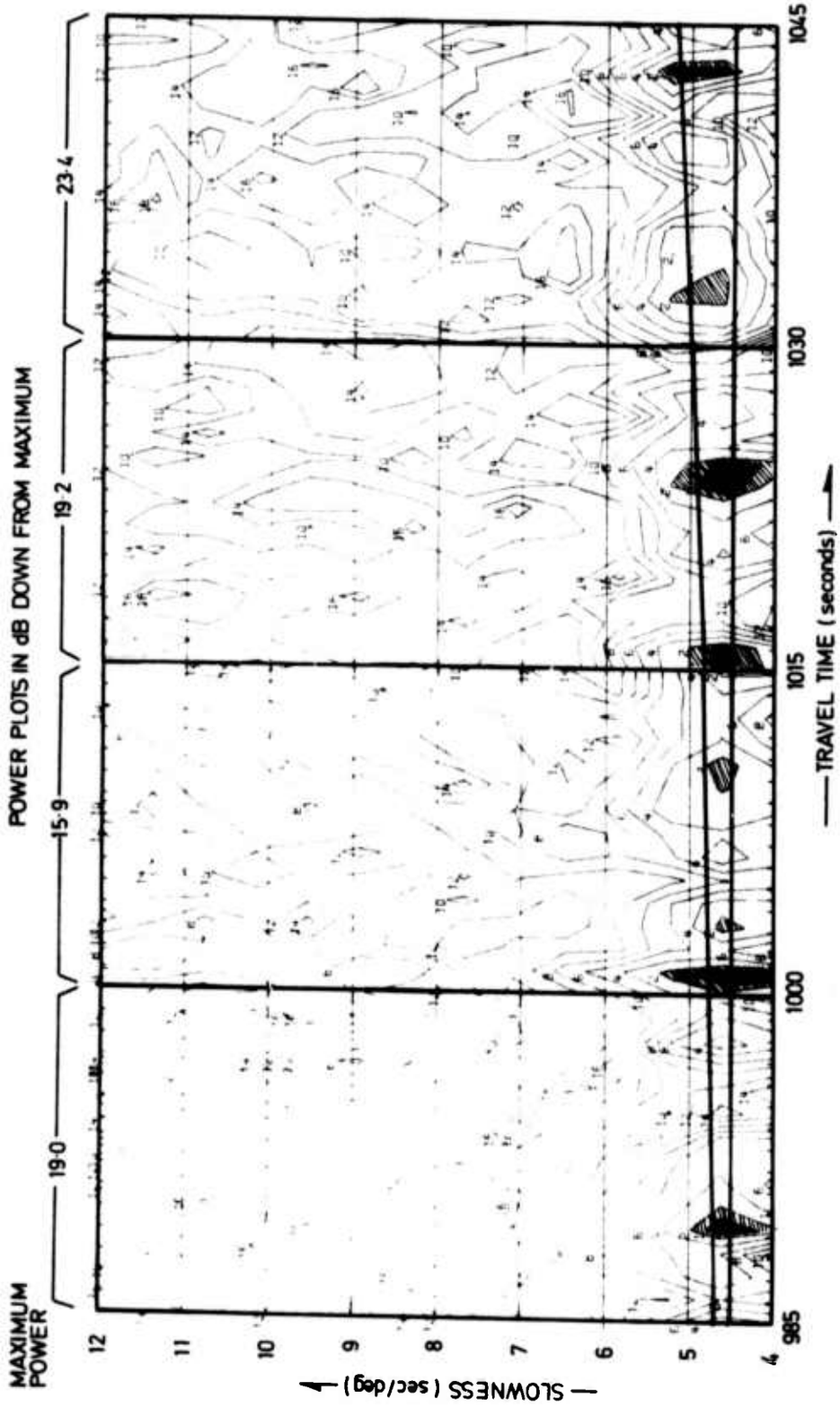

Fig 16. Caption and continuation of figure on following page.

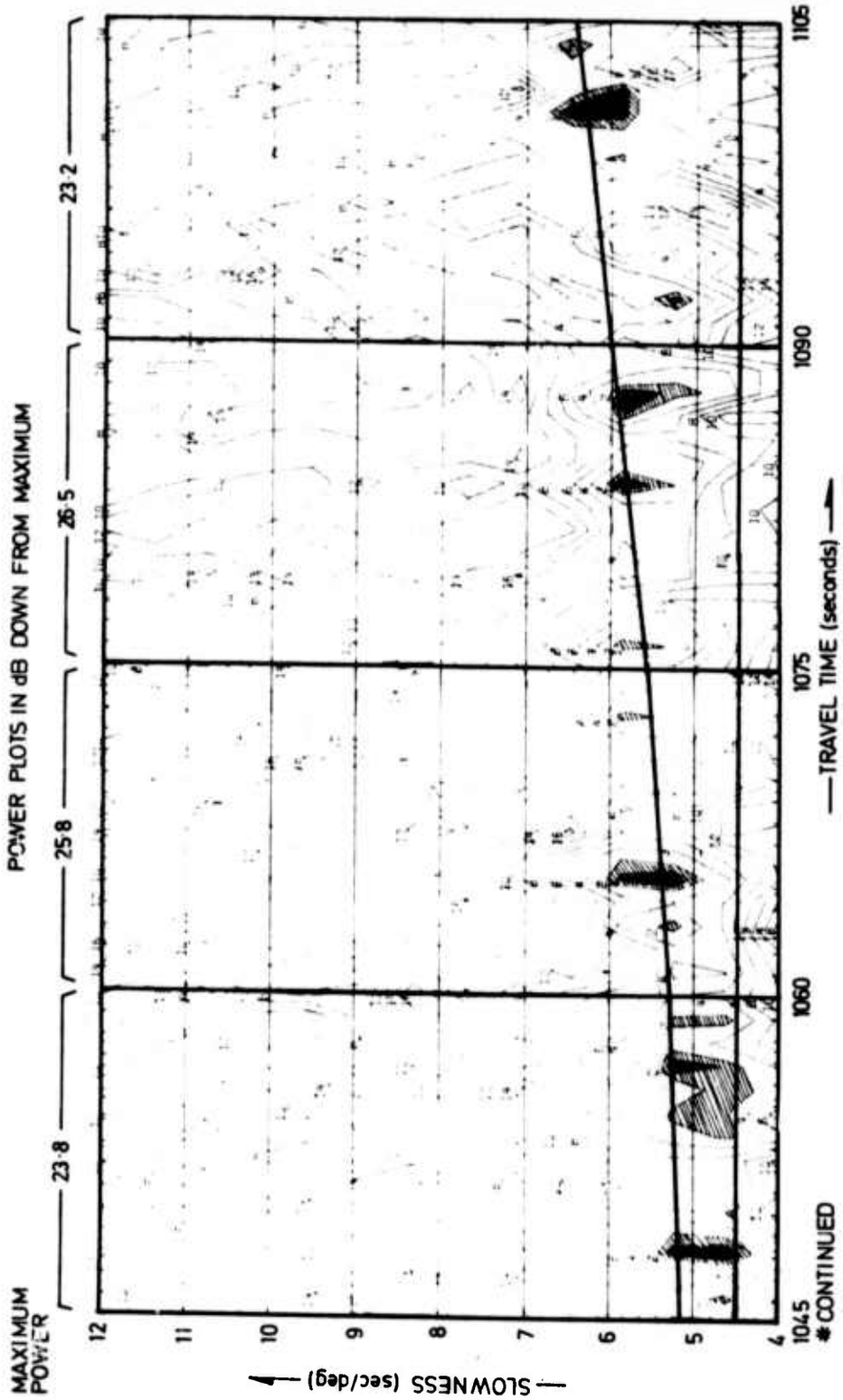

Fig. 16 Vespa-type plot of the distribution of power as a function of slowness and travel time for event 1. The Vespagram has been formed by averaging beam power values from 6 adjacent azimuths (in the range of $\pm 18^{\circ}$) for each slowness and each second of data. The data plotted is for a nominal azimuth of 246°, and the time axis is corrected for focal depth. Major power peaks are dotted (1 dB $\leq$ power $\leq$ dB) and hatched (2 dB $\leq$ power $\leq$ 1 dB), the power values being relative to the power maxima in the intervals indicated at the top of the figure. The bounds of slowness for the lower slowness group of arrivals for $\Delta=105^{\circ}$ for the Jeffreys velocity model are plotted (heavy lines) for comparison with the observed values. Note that the measured slownesses closely follow the theoretical upper bound line.

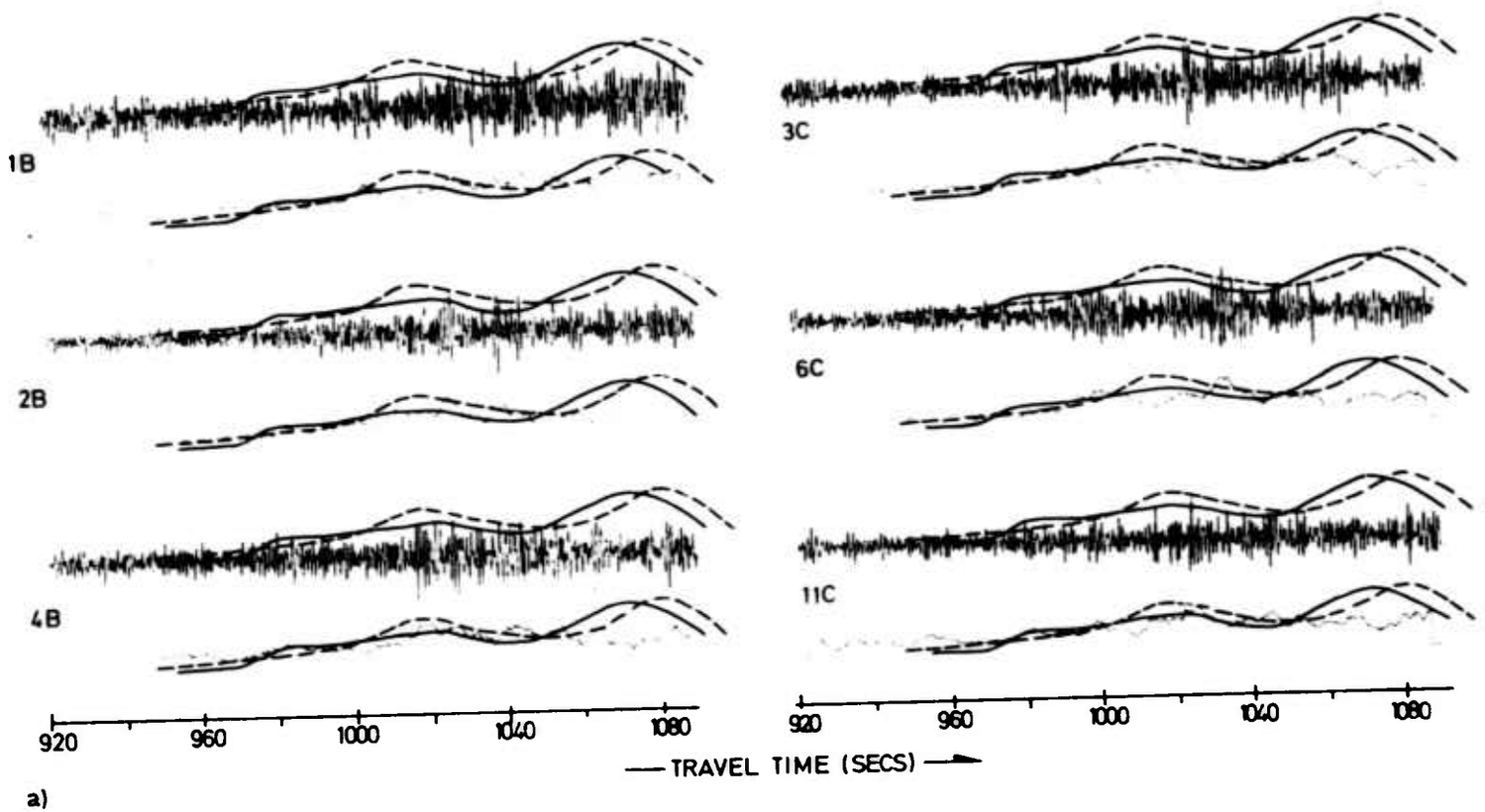

Fig. 17 a Seismogram and STA traces for Event 2. Details as in caption for Fig. 14.

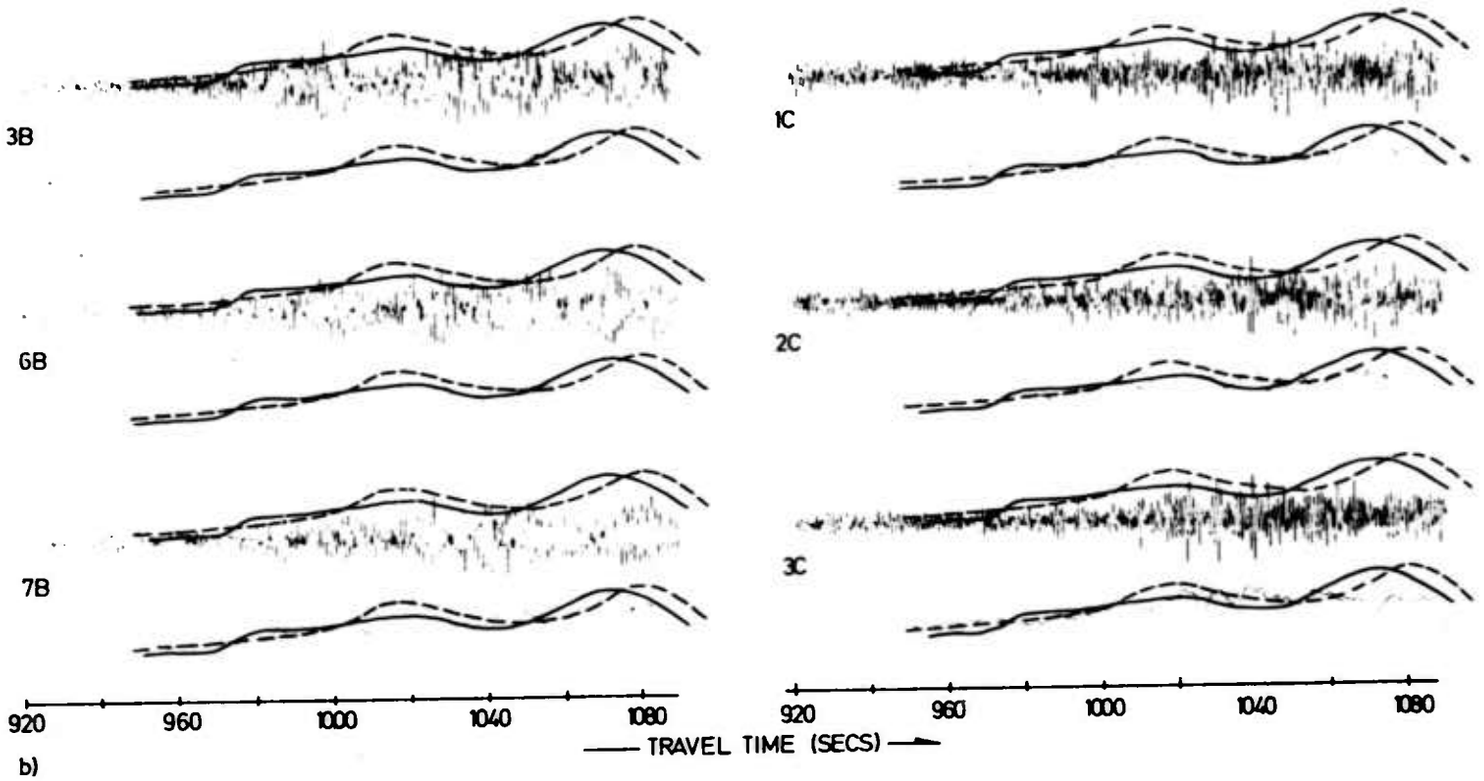

Fig. 17 b Seismogram and STA traces for Event 3. Details as in caption for Fig. 14.

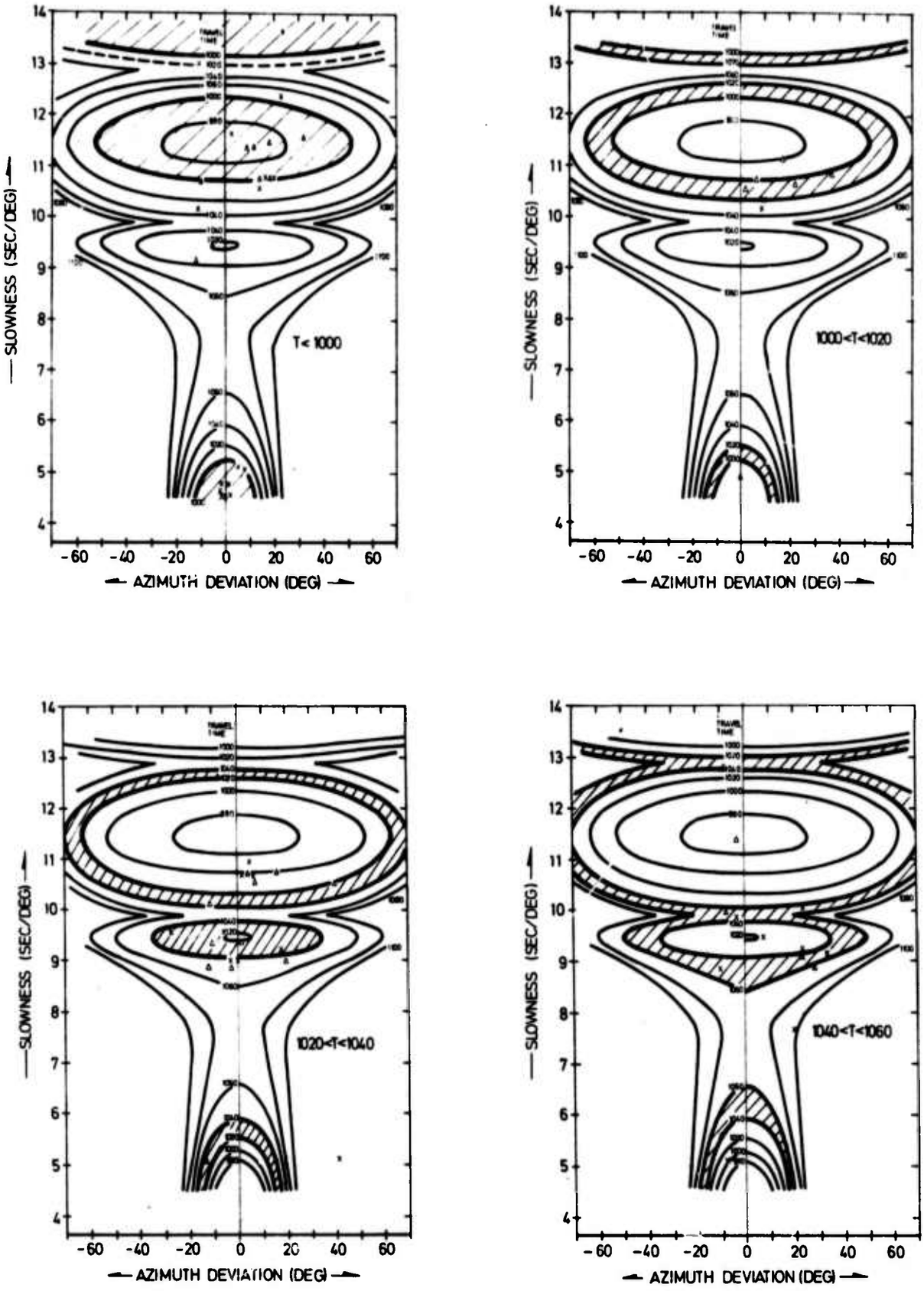

Fig 18. Caption and continuation of figure on following page

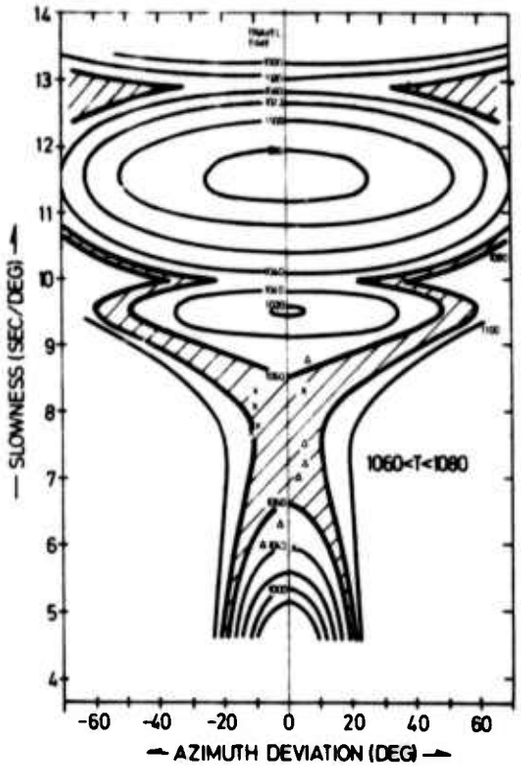

Fig. 18 Measured (s,Φ) values at NORSAR for event 2 (triangles) and event 3 (crosses) plotted in comparison with theoretical (s,Φ) values for $\Delta=100^{0}$ for the SMAK II model. The measured values are grouped in depth-corrected travel time intervals of 20 secs, and the theoretical (s,Φ) results appropriate to each of the time intervals are hatched on the appropriate frames of the figure. Note the wide spread of measured azimuths associated with higher slowness (s>7.5 s/deg) observations (cf. Fig. 11).

tions, and only 7 of the remaining observed values are in serious conflict with the theoretical results. In view of the considerable difficulties in making (s,Φ) measurements within the P coda, as evidenced by the paucity of published data, we regard the observational data as being in very satisfactory agreement with the theoretical expectations. Random interference effects between the various contributions together with distortion of the signal by structure beneath the array may account for the inconsistent observations, although we have not investigated this possibility in detail. Additional features of the data presented

which support the scattering interpretation of the PP precursor wave trains are the increase in the spread of the azimuthal observations associated with the higher slowness observations, and the gradual coalescing of the high and low slowness regimes with increasing time. The extent of the spread of the power in azimuth is also apparent in Fig. 11, as is the consistency with the theoretical curves included in this figure. Finally, we remark that the very low coherence in the highly energetic PP precursor wave trains analysed here is in itself quite significant support for the scattering interpretation.

8. DISCUSSION

Theoretical calculations for the assumed models indicate that on the linear scattering theory the total energies in the "higher" and "lower" slowness groups of scattered wave arrivals at a receiver are practically equal. However the ranges of slowness and azimuth for the lower slowness group are very much smaller than for the higher slowness group (see Figs. 2 and 5), and so the lower slowness group would be much more coherent at a receiver array. Thus, other things being equal, the highest scattered wave intensities would be expected to be associated with the lower slowness arrivals. These theoretical expectations are borne out well by the WRA data and the NORSAR data from region A (Fig. 7). In addition, while lower slowness PP precursors have been commonly observed (see, for example, references in introduction), only Wright (1972) has previously reported observations of the higher slowness group. We suggest that ob-

servations of the higher slowness group, such as the extensive NORSAR observations from region B (Fig. 7), are most likely to be made when the lower slowness group is relatively weak or absent. This could happen as a result of large-scale regional variations in the upper mantle scattering structure, and comparison of NORSAR (s,Φ) data from regions A and B is strong evidence for such regional variations. There is also a suggestion in the (s,Φ) data from region B (see Fig. 18) that scattering on the western side of the diametral azimuth is somewhat stronger than on the eastern side. We interpret the dominance of the higher slowness group in the NORSAR data from region B as offering strong evidence for the presence of widespread random irregularities in the vicinity of the Ural mountains, some 20^{o} to 30^{o} from NORSAR. This conclusion is broadly consistent with implications of the WRA data, which provides independent evidence for effective scattering in a similar region.

In the observed wave trains shown in Figures 12, 14 and 17, the mean amplitudes of the PP precursors are approximately equal to the amplitudes of the main PP phases. The corresponding theoretical precursor amplitudes for the model are only about a quarter of the amplitude of the PP phase. Increasing the assumed proportional r.m.s. variations in density and elastic parameters from 1% would increase the theoretical r.m.s. amplitudes of the scattered waves relative to the main PP (primary) phase proportionally. It is evident from the theoretical amplitude curves shown, however, that even for 1% variations a significant part of the energy in the primary P wave train would be transformed

into scattered waves in the assumed model (particularly for the shorter period waves), an effect not allowed for on the linear scattering theory. While this indicates a certain inadequacy of the linear theory in the present context, scrutiny of the theory shows that Eq. (1) may still be applied to model the scattering process if it is assumed that the energy in each narrow beam of primary wave rays entering the (thin) scattering layer is scattered so that the resultant relative directional intensity of the energy emerging from the layer may be approximated empirically by $\exp[-a^2\sin^2\phi/2]$, where ϕ denotes scattering angle and a is a constant. Further assuming ordinary ray theory to give the relative amplitudes of the primary waves entering the postulated scattering layer and the effects of geometrical spreading on the scattered waves after emerging from the layer (as in the linear theory), Eq. (1) would give the relative r.m.s. amplitudes of the resultant scattered waves of PP type arriving at a surface receiver in the assumed model. In these circumstances the kinematic characteristics of the scattered waves (i.e., slownesses, azimuths and arrival times) would be the same as for the linear theory, but the parameters Γ, k and σ appearing in Eq. (1) would not have any physical significance. The use of Eq. (1) to represent strong scattering effects thus amounts essentially to postulating a plausible directional intensity function for scattered waves emerging from each element of the postulated scattering layer rather than postulating the physical characteristics of the layer and deriving the consequent scattering effects. While in the former case there is no established connection between the characteristics of the postulated random medium and the consequent scattering

effects produced, this in no way affects our basic interpretation of the PP precursors. Notwithstanding all the various uncertainties involved, the extent of agreement between the observed and theoretical results presented strongly supports the scattering interpretation of PP precursors.

9. CONCLUSIONS

Seismic scattering by random inhomogeneities in the crust and upper mantle has been shown to account adequately for detailed observational data on precursors to PP from the WRA and NORSAR arrays. These data included principally onset times and duration, slowness, azimuth and amplitude variations of precursor wave trains. Many of these features find no explanation in any previously suggested interpretation of the precursors. A similar scattering interpretation accounts for precursors to PKPPKP having lead times less than about 90 seconds (King and Cleary, 1974; Haddon et al., 1975). Scattering also appears to account adequately for the entire short period teleseismic P coda (Cleary et al., 1974). With regard to the latter, the study of precursors to PP is important insofar as there seems little prospect of establishing unambiguously the relative contributions of various coda-generating mechanisms (e.g., Key, 1967, 1968; Husebye and Madariaga, 1970; Davies et al., 1971; Greenfield, 1971; Phinney et al., 1974) from studies of the coda between P and any precursor arrivals. The scattering interpretation of PP (and PKPPKP) precursors entirely removes the need for postulating sharp reflecting discontinuities in the uppermost few hundred kilometers of the crust and upper mantle.

REFERENCES

Aki, K., 1969. Analysis of the seismic coda of local earthquakes as scattered waves, J. Geophys. Res., 74: 615-631.

Aki, K., 1973. Scattering of P waves under the Montana Lasa, J. Geophys. Res., 78: 1334-1346.

Aki, K. and Chouet, B., 1974. Seismic coda of local earthquakes: source, attenuation and scattering effects, in press.

Angoran, Y. and Davies, D., 1972. Studies of PP and precursors to it, abstract only, Transactions, A.G.U., 53: 447.

Berteussen, K.A., 1975. Crustal structure and P-wave travel time anomalies at NORSAR, in press, J. of Geophys.

Berteussen, K.A. and Husebye, E.S., 1974. Amplitude pattern effects on NORSAR P-wave detectability, NORSAR Scientific Report 1-74/75: 52 pp.

Berteussen, K.A., Christoffersson, A., Husebye, E.S. and Dahle, A., 1974. Wave scattering theory in analysis of P-wave anomalies at NORSAR and LASA, Proc. NATO ASI, Exploitation of Seismograph Networks, Sandefjord, Norway.

Bolt, B.A., 1970. P_dP and PKiKP waves and diffracted P_cP waves, Geophys. J.R. astr. Soc., 20: 367-382.

Bolt, B.A., O'Neill, M. and Qamar, A., 1968. Seismic waves near 110°: is structure in core or upper mantle responsible? Geophys. J.R.astr. Soc., 16: 475-487.

Bullen, K.E., 1963. Introduction to the Theory of Seismology, University Press, Cambridge.

Capon, J., 1974. Characterization of crust and upper mantle structure under LASA as a random medium, Bull. Seism. Soc. Am., 64: 235-266.

Capon, J. and Berteussen, K.A., 1974. A random medium analysis of crust and upper mantle structure under NORSAR, Geophys. Res. Lett., 1, 7: 327-328.

Capon, J. and Davies, D., 1971. Pattern recognition techniques for the interpretation of Vespagrams and Beamsplit data, Semiannual Tech. Summary, M.I.T., Lincoln Lab, June 30: 38-40 and 49-51.

Cleary, J.R. and Haddon, R.A.W., 1972. Seismic wave scattering near the core-mantle boundary: a new interpretation of precursors to PKIKP, Nature, 240, Dec. 29th: 549-551.

Cleary, J.R. and Haddon, R.A.W., 1973. P wave scattering in the Earth's crust and upper mantle, paper presented to meeting of I.A.S.P.E.I., Lima, Peru.

Cleary, J.R., King, D.W. and Haddon, R.A.W., 1974. Seismic wave scattering in the Earth's crust and upper mantle, submitted for publication.

Dainty, A.M. and Anderson, K.R., 1972. Seismic scattering in the Moon and the Earth abstract only, Transactions, A.G.U., 53: 446.

Davies, D., 1971. Coda coherence - a distinction between different mantle regions, Semiannual Tech. Summary, M.I.T., Lincoln Lab, June 30: 20-21 and 28-31.

Davies, D. and Frasier,C.W., 1970. A Chinese puzzle, in Seismic Discrimination, Semiannual Tech. Summary, M.I.T., Lincoln Lab., December 31.

Davies, D., Kelly, E.J. and Filson, J.R., 1971. Vespa process for analysis of seismic signals, Nature, Physical Science, 232, July 5th: 8-13.

Doornbos, D.J. and Husebye, E.S., 1972. Array analysis of PKP phases and their precursors, Phys. Earth Planet. Int., 5: 387-399.

Doornbos, D.J. and Vlaar, N.J., 1973. Regions of seismic wave scattering in the Earth's mantle and precursors to PKP, Nature, Physical Science, 243, May 28: 58-61.

Greenfield, R.J., 1971. Short-period P wave generation by Rayleigh-wave scattering at Novaya Zemlya, J. Geophys. Res., 76: 7988-8002.

Gutowski, P.R. and Kanasewich, E.R., 1974. Velocity spectral evidence of upper mantle discontinuities, Geophys. J.R. astr. Soc., 36: 21-32.

Haddon, R.A.W., 1972. Corrugations on the mantle-core boundary or transition layers between inner and outer cores?, abstract only, Transactions, A.G.U., 53: 600.

Haddon, R.A.W., 1974. Scattering of seismic body waves by small random inhomogeneities in the earth, submitted for publication.

Haddon, R.A.W. and Cleary, J.R., 1974. Evidence for scattering of seismic PKP waves near the mantle-core boundary, Phys. Earth Planet. Int., 8: 211-234.

Haddon, R.A.W., Husebye, E.S. and King, D.W., 1975. Precursors to PKPPKP, manuscript in preparation.

Husebye, E.S. and Madariaga, R., 1970. The origin of precursors to core waves, Bull. Seism. Soc. Am., 60: 939-952.

Jeffreys, H., 1939. The times of P, S and SKS and the velocities of P and S, Mon. Not. R.astr. Soc., Geophys. Suppl., 4: 498-533.

Jeffreys, H. and Bullen, K.E., 1940. Seismological Tables, British Association for the Advancement of Science, Gray Milne Trust, London: 50 pp.

Kelly, E.J., 1967. Response of seismic arrays to wide-band signals, Tech. Note 1967-30, Lincoln Lab, M.I.T., Mass.: 47 pp.

Key, F.A., 1967. Signal-generated noise at the Eskdalemuir Seismometer Array Station, Bull. Seism. Soc. Am., 57: 27-37.

Key, F.A., 1968. Some observations and analyses of signal-generated noise, Geophys. J.R.astr. Soc., 15: 377-392.

King, D.W. and Cleary, J.R., 1974. A note on the interpretation of precursors to PKPPKP, Bull. Seism. Soc. Am., 64: 721-723.

King, D.W., Haddon, R.A.W. and Cleary, J.R., 1973. Evidence for seismic wave scattering in the D" layer, Earth Planet. Sci. Lett., 20: 353-356.

King, D.W., Haddon, R.A.W. and Cleary, J.R., 1974. Array analysis of precursors to PKIKP in the distance range 128° to 142°, Geophys. J.R. astr. Soc., 37: 157-173.

Mereu, R.F., Simpson, D.W. and King, D.W., 1974. Q and its effect on the observation of upper mantle travel time branches, Earth Planet. Sci. Lett., 21: 439-447.

Nguyen-Hai, 1963. Propagation des ondes longitidinales dans le noyau terrestre, Annales de Géophysique, 19, 4: 285-346.

Phinney, R.A., Dahlen, F.A. and Malin, P., 1974. Scattering mechanisms for the spectra of P and S codas, Trans. A.G.U., April, abstract only.

Steinberg, B.D., 1971. On teleseismic beam formation by very large arrays, Bull. Seism. Soc. Am., 61: 983-992.

Wright, C., 1972. Array studies of seismic waves arriving between P and PP in the distance range 90° to 115°, Bull. Seism. Soc. Am., 62: 385-400.

Wright, C. and Muirhead, K.J., 1969. Longitudinal waves from the Novaya Zemlya nuclear explosion of October 27 1966, recorded at the Warramunga seismic array, J. Geophys. Res., 74: 2034-2047.